Received: 27 March 2024 | Revised: 30 August 2024 | Accepted: 4 September 2024

DOI: 10.1111/gcb.17509

Global Change Biology WILEY

RESEARCH ARTICLE

Eddy covariance measurements reveal a decreased carbon sequestration strength 2010–2022 in an African semiarid savanna

Aleksander Wieckowski[1] | Patrik Vestin[1] | Jonas Ardö[1] | Olivier Roupsard[2,3,4] | Ousmane Ndiaye[5] | Ousmane Diatta[5] | Seydina Ba[4,6] | Yélognissè Agbohessou[2,3] | Rasmus Fensholt[7] | Wim Verbruggen[7] | Haftay Hailu Gebremedhn[8] | Torbern Tagesson[1]

[1]Department of Physical Geography and Ecosystem Science, Lund University, Lund, Sweden

[2]CIRAD, UMR Eco&Sols, Dakar, Senegal

[3]Eco&Sols, CIRAD, INRAE, Institut Agro, IRD, Univ Montpellier, Montpellier, France

[4]LMI IESOL, Centre IRD-ISRA de Bel Air, Dakar, Senegal

[5]Institut Sénégalais de Recherches Agricoles, Dakar, Senegal

[6]Faculté Des Sciences et Techniques, Université Cheikh Anta Diop, Dakar, Senegal

[7]Department of Geosciences and Natural Resource Management, University of Copenhagen, Copenhagen, Denmark

[8]African Center of Excellence for Climate-Smart Agriculture and Biodiversity, Haramaya University, Dire Dawa, Ethiopia

Correspondence
Aleksander Wieckowski, Department of Physical Geography and Ecosystem Science, Lund University, Sölvegatan 12, SE-223 62 Lund, Sweden.
Email: aleksander.wieckowski@nateko.lu.se

Funding information
European Union, Grant/Award Number: FOOD/2019/410-169; Danmarks Frie Forskningsfond, Grant/Award Number: 10.46540/2032-00026B; Svenska Forskningsrådet Formas, Grant/Award Number: Dnr 2023-02436 and Dnr 2021-00644; Villum Fonden, Grant/Award Number: 37465; Swedish National Space Agency, Grant/Award Number: Dnr 2021-00111 and Dnr 2023-00144; Lunds Universitet, Grant/Award Number: Dnr 2012/377

Abstract

Monitoring the changes of ecosystem functioning is pivotal for understanding the global carbon cycle. Despite its size and contribution to the global carbon cycle, Africa is largely understudied in regard to ongoing changes of its ecosystem functioning and their responses to climate change. One of the reasons is the lack of long-term in situ data. Here, we use eddy covariance to quantify the net ecosystem exchange (NEE) and its components—gross primary production (GPP) and ecosystem respiration (R_{eco}) for years 2010–2022 for a Sahelian semiarid savanna to study trends in the fluxes. Significant negative trends were found for NEE ($12.7 \pm 2.8\,g\,C\,m^2\,year^{-1}$), GPP ($39.6 \pm 7.9\,g\,C\,m^2\,year^{-1}$), and R_{eco} ($32.2 \pm 8.9\,g\,C\,m^2\,year^{-1}$). We found that NEE decreased by 60% over the study period, and this decrease was mainly caused by stronger negative trends in rainy season GPP than in R_{eco}. Additionally, we observed strong increasing trends in vapor pressure deficit, but no trends in rainfall or soil water content. Thus, a proposed explanation for the decrease in carbon sink strength is increasing atmospheric dryness. The warming climate in the Sahel, coupled with increasing evaporative demand, may thus lead to decreased GPP levels across this biome, and lowering its CO_2 sequestration.

KEYWORDS
carbon loss, climate change, eddy covariance, rainfall, Sahel, semiarid savanna, vapor pressure deficit, water availability

1 | INTRODUCTION

Terrestrial ecosystems sequester approximately 31% of the anthropogenic carbon emissions, being an essential ecosystem service mitigating climate change (Friedlingstein et al., 2023). This carbon sink was found to increase in strength globally (Ruehr et al., 2023), and it has been shown that semiarid regions play an increasingly important role representing the main biome driving global long-term trends and inter-annual variability of carbon sequestration (Ahlström et al., 2015; Poulter et al., 2014). However, the long-term variability of land–atmosphere carbon exchange processes of these semiarid savannas is still not well understood (Rybchak et al., 2024).

The African Sahel is one of the world's largest semiarid savanna areas, being a transition zone situated amidst the Sahara Desert to the north and the humid Sudanian savanna to the south. It is characterized by a sparse cover of trees and shrubs with an understory dominated by grasses and forbs (Tagesson, Fensholt, & Guiro, 2015; Verbruggen et al., 2021). This region has been affected by severe droughts impacting ecosystem services important for local livelihoods, such as crop production, grazing, and water availability (Abdi et al., 2014; Adaawen et al., 2019; Booker et al., 2013; Gebremedhn et al., 2023; Sanni et al., 2012; Seid et al., 2016). Rainfall is the primary driver of vegetation growth in the Sahel, which makes the ecosystem responses vulnerable to the effects of climate change, such as increased drought frequency (Hickler et al., 2005; Mortimore, 2010) and increased evaporative demand (Vicente-Serrano et al., 2020). In the past decades, an increased frequency of extreme rainfall events, alongside a decreased a number of rainy days, has been observed (Taylor et al., 2017). Additionally, there has been a cropland expansion, alongside degradation of natural ecosystems (Souverijns et al., 2020). Therefore, ongoing land use and climate changes might be affecting ecosystem functioning and carbon cycling.

It has also been found that the region is experiencing an increase in net land carbon sink strength (Friedlingstein et al., 2023), satellite observed leaf area (Ruehr et al., 2023) and greenness (Jiang et al., 2022; Zeng et al., 2023). However, these are based on satellite observations or model simulations, and a major restriction of our understanding of changes of ecosystem functioning in the Sahel, and other tropical semiarid areas, is the lack of long-term in situ data records (Zscheischler et al., 2017). Long-term land–atmosphere exchange measurements promote the understanding of the dynamic responses of the carbon exchange processes to changing environmental conditions and are pivotal for the parameterization and evaluation of remote sensing products and dynamic vegetation models (Gu et al., 2018). Hence, there is an increasing demand for field observations of environmental variables and carbon exchange processes, especially from the tropical regions (Gamon et al., 2010; Kattge et al., 2020; Pastorello et al., 2020).

The net ecosystem exchange (NEE) of CO_2 is the balance between the CO_2 assimilated by the vegetation (gross primary production; GPP) and carbon released via respiratory processes (heterotrophic and autotrophic respiration; combined referred to as ecosystem respiration; R_{eco}). There have been a few studies investigating the CO_2 exchange processes using the eddy covariance (EC) technique in the Sahel (Ardö et al., 2008; Boulain et al., 2009; Hanan et al., 1996; Mauder et al., 2021; Merbold et al., 2009; Tagesson, Fensholt, et al., 2016), but none of these are based on decadal or longer scale time series, required for studies of trends and of the controlling factors of long-term variability.

Tagesson, Fensholt, Cropley, et al. (2015) and Tagesson, Ardö, et al. (2016) used the EC technique to study drivers of the diurnal and seasonal dynamics of the land–atmosphere CO_2 exchange processes at the Dahra field site, a grazed semiarid savanna ecosystem located in Senegal. They found that the dynamics at these fine temporal resolutions were most strongly governed by photosynthetically active radiation (PAR), soil moisture, and vapor pressure deficit (VPD). However, these ecosystem-scale CO_2 flux measurements have now been conducted for an additional 9 years (13 years in total). This time series of CO_2 fluxes in combination with long-term data of hydro-meteorological conditions allows us to assess the dynamics of the CO_2 fluxes on inter-annual scale and to study how these are influenced by the ecosystem properties and changes in environmental conditions. Therefore, this study was designed to answer the following research questions:

(i) What are the trends of measured NEE, GPP, R_{eco}, for the years 2010–2022 in a Sahelian semiarid savanna?
(ii) Which external and internal drivers (air and soil temperature, PAR, VPD, rainfall, soil water content (SWC), greenness (the normalized difference vegetation index [NDVI], rainy season length, water use efficiency [WUE], and inherent WUE [IWUE]) are likely to affect the observed NEE, GPP, R_{eco} trends?

2 | MATERIALS AND METHODS

2.1 | Site description

The measurements were conducted at the Dahra field site in the Sahelian zone of Senegal (15°24′10″ N, 15°25′56″ W, elevation 40 m) (Figure 1). The site is a grazed semiarid savanna grassland. Annual mean rainfall is 416 mm (for the period 1951–2003) of which more than 95% of the rain falls during the rainy season (July–October), with August being the wettest month (Agence Nationale de l'Aviation Civile et de la Météorologie, Senegal). The site also experiences a decreasing trend in rainfall since the 1950s (Supporting Information subsection S1). Annual air temperature (for the period 1951–2003) is 29°C; May has the highest mean monthly temperature (32°C) and January the lowest (25°C). South-westerly winds dominate during the rainy season, whereas north-easterly winds dominate during the dry season. The site is a low tree and shrub savanna with ~3% tree cover (Rasmussen et al., 2011). Most abundant tree species are *Balanites aegyptiaca*, *Vachellia tortilis*, *Senegalia senegal*, while the ground vegetation primarily consists of annual C4 grasses (e.g., *Cenchrus biflorus*, *Eragrostis tremula*, *Aristida adscensionis*, *Dactyloctenium aegyptium*) (Tagesson, Fensholt, & Guiro, 2015) and forbs (e.g., *Diodella samentosa* and *Zornia glochidiata*) (Gebremedhn et al., 2023). The soil is sandy

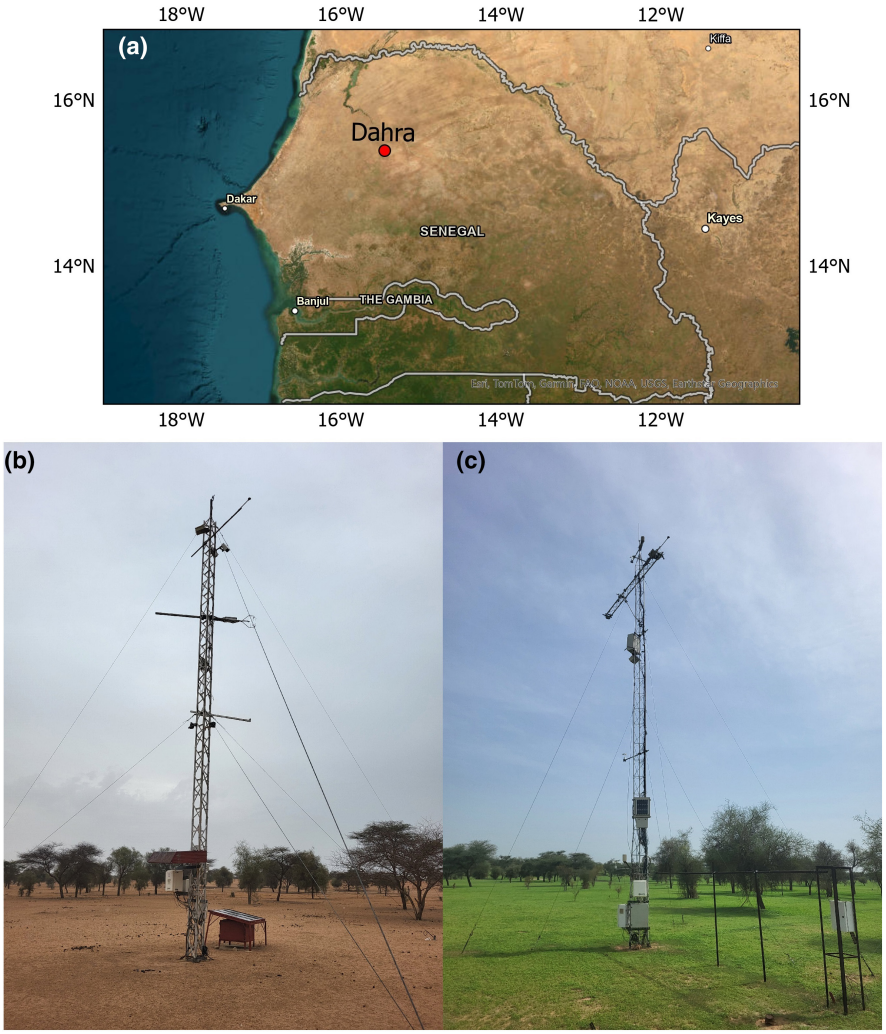

FIGURE 1 The study location. (a) Location of the Dahra field site in Senegal; (b) the eddy covariance tower during the dry season; and (c) the meteorological tower during the rainy season. Map lines delineate study areas and do not necessarily depict accepted national boundaries.

luvic arenosol with negligible amounts of organic material and low clay content (Clay = 0.35%, silt = 4.61%, and sand = 95.04%) (Tagesson, Fensholt, & Guiro, 2001). The instrumental setup consists of two towers: one with an EC system for CO_2, H_2O, and energy flux measurement, and one with meteorological sensors (Figure 1). The detailed sensor setup is described in Tagesson, Fensholt, and Guiro (2015).

2.2 | EC and environmental data

NEE (μmol CO_2 $m^{-2}s^{-1}$) and latent heat (LE) ($W m^{-2}$) were measured between August 8, 2010 and December 31, 2022 using an EC system installed at 9-m height. Negative NEE represents a net uptake of CO_2 from the atmosphere, thus a sink in a given time period. We used a Gill R3 Ultrasonic Anemometer (Gill instruments Ltd, Lymington, UK) and an open-path CO_2/H_2O infrared gas analyzer (LI-7500, LI-COR Inc. Lincoln, NE, USA) between 2010 and 2017, and a closed-path EC155 CO_2/H_2O infrared gas analyzer in combination with a CSAT3A sonic anemometer (combined referred to as the CPEC 200 system, Campbell Scientific, Logan, UT, USA) 2019–2022. The analyzers had a 20 and 15 cm horizontal and a 24 and −5 cm vertical separation from the anemometer, for the open-path and closed-path analyzers, respectively. The open-path analyzer was also inclined 29° from vertical. Data were captured at a rate of 20 and 10 Hz for the open-path and closed-path measurements, respectively. The open-path gas analyzer was calibrated every 4 weeks and the closed path once per year.

The data processing included de-spiking (Vickers & Mahrt, 1997), 2D coordinate rotation (Wilczak et al., 2001), time lag removal between anemometer and gas analyzer by covariance maximization (Fan et al., 1990), linear detrending (Moncrieff et al., 2005), and for the open-path analyzer compensation for density fluctuations (Webb et al., 1980) in EddyPro (LI-COR Inc. Lincoln, NE, USA). The fluxes were adjusted for the effects of low- and high-pass filtering (Moncrieff et al., 1997, 2005). Additionally, statistical tests for skewness and kurtosis were used for filtering (Vickers & Mahrt, 1997). Data were quality filtered based on tests for steady-state conditions and developed turbulent conditions (Foken et al., 2004). For the open-path analyzer, data collected during rainfall events were rejected. The filtered data coverage of the measured period was 50.4%. However, there were additional large gaps between November 5, 2010 and July 17, 2011, January 11, 2013 to July 7, 2013, and throughout 2014 and 2018 caused by broken sensors, maintenance, and the sensor shift. In the end, 32.7% of the full NEE time series in 2010–2022 was captured, consisting of 51.1% data

captured in rainy season and 24.4% in the dry season (26.7%, 18.7%, 46.3% for LE, respectively).

Hydrometeorological variables were measured continuously except for during the periods from October26, 2010 to February 25, 2011, and March 2, 2014 to March 22, 2014, due to technical issues. Measured variables were air (T_{air}) and soil temperature (T_{soil}) (°C) measured at 2 and −0.10 m, respectively, relative humidity (RH) (%) measured at 2 m, SWC (%) measured at 0.05 m, PAR (μmol $m^{-2} s^{-1}$) measured at 10.5 m, and rainfall (mm) measured at 2 m with four rain gauges. The detailed sensor setup is described in Tagesson, Fensholt, Cropley, et al. (2015). Incoming and reflected red and near-infrared radiation was also measured at 10.5 m and used to calculate the NDVI (Tucker, 1979). All sensors were connected to CR1000 data loggers in combination with a multiplexer (Campbell Scientific Inc., Logan, UT, USA), and data were sampled every 30 s and stored as 15 min averages (sum for rainfall). VPD (hPa) was calculated from T_{air} and RH (Wutzler et al., 2018).

2.3 | Gap filling and partitioning of the measured CO_2 and water fluxes

The NEE time series was filtered for low friction velocity (u_*), gap-filled and partitioned using ReddyProc (Wutzler et al., 2018). For the u_* filtering, we used the method of Papale et al. (2006). We used the marginal distribution sampling (MDS) algorithm described in Reichstein et al. (2005) for the gap filling, whereas the partitioning into GPP and R_{eco} was done using the day-time algorithm (Lasslop et al., 2010). Low-quality data in the gap-filled NEE, GPP, R_{eco}, and LE time series were then excluded using the quality flag threshold of >1 (Wutzler et al., 2018). This first gap-filled dataset still consisted of both short and long data gaps and the subsequent gap-filling processing steps were therefore applied: (1) up to 7 days long gaps in environmental variables were filled using an 8-day moving window for the same time of the day. (2) Longer gaps in the environmental variables were filled using a mean value for a given time and day of the year, calculated from the full time series 2010–2022. (3) Remaining gaps in the NEE, GPP, R_{eco}, and LE time series were filled using the average outputs from random forest (RF) simulations. The RF model was implemented in Python Scikit-Learn module and included 1000 trees (Breiman, 2001; Pedregosa et al., 2011). Other parameters of RF were set as default, that is, no maximal depth of the tree, two samples required to split a node and one sample required at each node (Breiman, 2001). We used PAR, VPD, and T_{air} as explanatory variables, and non-gapfilled GPP, R_{eco}, NEE, and LE as training data. We obtained good fits for gap-filled NEE, GPP, R_{eco}, and LE as predicted by RF and by ReddyProc (Supporting Information subsection S2).

2.4 | Annual budgets and their uncertainties

Annual budgets of GPP, NEE, and R_{eco} were calculated as sums of half-hourly values for each year. This was followed by an analysis of uncertainty in the annual budgets. This analysis does not take all uncertainties into account, but does provide an estimate of the main errors within the flux budgets. Random errors in sampling of flux measurements may occur due to the stochasticity of turbulence; thus, we calculated variance of the covariance between CO_2 concentrations and vertical wind speed to quantify random uncertainty. This was done in EddyPro (LI-COR Inc. Lincoln, USA), using the method of Finkelstein and Sims (2001). We estimated the uncertainty related to the selection of the u_* thresholds as different u_* thresholds will yield different contributions of gap filling to the carbon flux budgets. We ran 200 bootstrap simulations to generate artificial replicates of the dataset and for each replicate a u_* threshold was estimated. The 5th, 50th, and 95th percentile of these 200 u_* threshold levels were used for estimating annual budgets of NEE, GPP, and R_{eco}, where the standard deviations of these three budgets provides the uncertainty related to the u_* filtering threshold (Wutzler et al., 2018). Subsequently, we inferred the uncertainty of the MDS and RF gap-filling algorithms using bootstrap simulations with 200 iterations (Wutzler et al., 2018). Uncertainty was calculated by calculating the standard deviation of the annual budgets generated with these 200 iterations. The total sum of the uncertainties from these sources (u_{total}) were estimated as:

$$u_{total} = \sqrt{u_{random}^2 + u_{u_*}^2 + u_{MDS}^2 + u_{RF}^2},$$

constituted by random uncertainties (u_{random}), u_* threshold induced uncertainties (u_{u_*}), and uncertainties from the gap filling of the MDS algorithm (u_{MDS}) and the RF simulations (u_{RF}).

2.5 | Data analysis

2.5.1 | Trends in the CO_2 flux budgets and in the environmental conditions 2010–2022

To study contributions of the dry and rainy season to the annual budgets of NEE, GPP, and R_{eco}, we extracted the data for the rainy season based on the first occurrence of at least 10 mm cumulative rainfall within 7 days after 1st of May, followed by a total of 20 mm rainfall within the next 20 days. The end of the rainy season was defined as the day of 20 consecutive days with cumulated rainfall less than 10 mm after 1st of September 1. The remaining data were treated as dry season observations. We then fitted ordinary least square linear regressions to estimate trends 2010–2022 in the annual and seasonal flux budgets, and in the environmental variable means: VPD, T_{air}, T_{soil}, PAR, SWC, NDVI and sums: rainfall, and rainy season length. Despite 13 years being too short of a period to study actual climate trends, it is included for studying their relationship with the CO_2 flux trends.

2.5.2 | Drivers of the changes in the CO_2 flux budgets 2010–2022

To disentangle the relationships between the GPP and R_{eco} budgets and VPD, T_{air}, PAR, SWC, and rainfall, we used a structural equation

model (SEM). In the analysis, both the fluxes and the environmental variables were binned as averages (sums for rainfall) for each given subset (i.e., rainy season, dry season, and full annual dataset). NEE is a result of the interplay between GPP and R_{eco}, and thereby rather driven by the causal mechanisms driving GPP and R_{eco}. We thereby excluded NEE from this analysis. For this analysis, we used absolute values of GPP instead of negative to improve the readability of the analysis. SEM is a multivariate statistical method that incorporate factor analysis, path analysis, and maximum likelihood estimation (Grace & Bollen, 2005; Wang et al., 2018). It is a method commonly used for disentangling the drivers of CO_2 fluxes (Ding et al., 2024; Flores-Rentería et al., 2023; Ma et al., 2024; Perez-Quezada et al., 2024; Wang et al., 2023). The SEM helps to understand and identify the direct and indirect effects of driving variables on CO_2 fluxes and the significance of those. For this purpose, we used the R package "lavaan" (Rosseel, 2012). Variables were standardized by subtracting the mean from each observation and divided by standard deviation. The path coefficients were standardized partial linear regression coefficients, representing the relative strength of a given relationship. We first considered a full model with all possible pathways and then sequentially eliminated nonsignificant pathways ($p > .05$) until obtaining the final model. To evaluate the model, we employed the following indices: chi-squared (χ^2), root mean square error of approximation (RMSEA), Comparative Fit Index (CFI), and Tuck–Lewis Index (TLI). The model is considered satisfactory if RMSEA is smaller than .05, the chi-square test is insignificant ($p > .05$) (Wang et al., 2024), CFI is greater than .95 and TLI is greater than .9 (Fan et al., 2016). We also did a principal component analysis not included in the main text, as it showed similar results as the SEM analysis (Supporting Information subsection S3).

Pearson correlation coefficients were also quantified to test how closely the GPP, R_{eco}, and NEE budgets were linearly correlated with the environmental variables VPD, T_{air}, T_{soil}, PAR, SWC, NDVI, rainfall, and rainy season length. Since NDVI and rainy season length are not physical drivers, we did not consider them appropriate for the SEM analysis. Thus, this analysis was mainly included to quantify how closely variables not included in the SEM analysis were related to the CO_2 flux budgets.

2.5.3 | Trends of WUE and IWUE to distinguish between responses of herbaceous vegetation and trees to the atmospheric drying

Ecosystem-scale WUE is a ratio of CO_2 assimilated via GPP to the loss of water via evapotranspiration (ET) (Beer et al., 2009). It is a critical metric to measure the trade-off between carbon uptake and water loss of terrestrial ecosystems in response to environmental changes (Niu et al., 2011). During the dry season in Sahelian semiarid savanna, the most important active component contributing to the CO_2 exchange is the trees (Agbohessou et al., 2023). At the end of the dry season (we used the last 3 months before the start of rainy season), minimal evaporation takes place; therefore, the small observed ET is mainly due to the transpiration of the evergreen trees (Nelson et al., 2018). Thus, observed changes of WUE during this part of the year provide information about the responses of tree activity to the changing environmental conditions, such as atmospheric drought (Grossiord et al., 2017). Assuming the density of water is constant at $1000\,kg\,m^{-3}$, LE fluxes can be converted to ET by dividing LE by the heat of vaporization ($\lambda = 2.501 - 0.00236 \times T_{air}$, where λ is in $MJ\,kg^{-1}$ and T_{air} is in °C) (Ding et al., 2010). WUE was then calculated as:

$$WUE = GPP / ET.$$

However, the standard WUE does not consider the evaporative demand of the atmosphere known to affect both GPP and ET (Beer et al., 2009). Beer et al. (2009) proposed to use an IWUE, where VPD is included to account for this effect. IWUE can therefore be used in relation to WUE to account for individual effect of VPD changes on long-term ecosystem responses. It is calculated as:

$$IWUE = GPP \times VPD / ET.$$

We then fitted ordinary least square linear regressions to estimate trends 2010–2022 in the annual and seasonal WUE and IWUE estimates.

3 | RESULTS

3.1 | Environmental conditions

During 2010–2022, mean annual temperature at the Dahra field site was 28.6°C, with December–February being the coldest, and April–June being the hottest months (Figure 2). The warmest months also had the highest incoming PAR (Figure 2). Average annual rainfall 2010–2022 was 379 mm with highest recordings in 2010 (637 mm) and the lowest in 2018 (260 mm). A significant increasing linear trend 2010–2022 was observed for VPD (Figure 3). No trends were observed in neither rainfall nor in SWC 2010–2022 (Figure 3).

3.2 | Land–atmosphere exchange of CO_2

NEE had strong seasonal variations with levels close to zero (−6 to 5 μmol $CO_2\,m^{-2}\,s^{-1}$) during the dry season, followed by strong emission bursts during the start of the rainy season (up to 16 μmol $CO_2\,m^{-2}\,s^{-1}$) and strong uptake levels during the middle of the rainy season (up to −46 μmol $CO_2\,m^{-2}\,s^{-1}$) (Figure 2).

The savanna ecosystem acted as a carbon sink for all years with an average annual NEE budget ($\pm u_{total}$) of $-180 \pm 29\,g\,C\,m^{-2}\,year^{-1}$, but with a large interannual variability (standard deviation of annual budgets: $58\,g\,C\,m^{-2}\,year^{-1}$; range -265 ± 39 to $-57 \pm 19\,g\,C\,m^{-2}\,year^{-1}$) (Table 1; Figure 4). Large differences of the cumulative NEE between years were observed during the dry season (average: $-54 \pm 9\,g\,C\,m^{-2}$; range from -115 ± 9 to $29 \pm 10\,g\,C\,m^{-2}$) (Table 1). There were also large differences in the rainy season budgets, with an average cumulative NEE of $-126 \pm 22\,g\,C\,m^{-2}$ and a range from $-205 \pm 31\,g\,C\,m^{-2}$ to -68 ± 15.

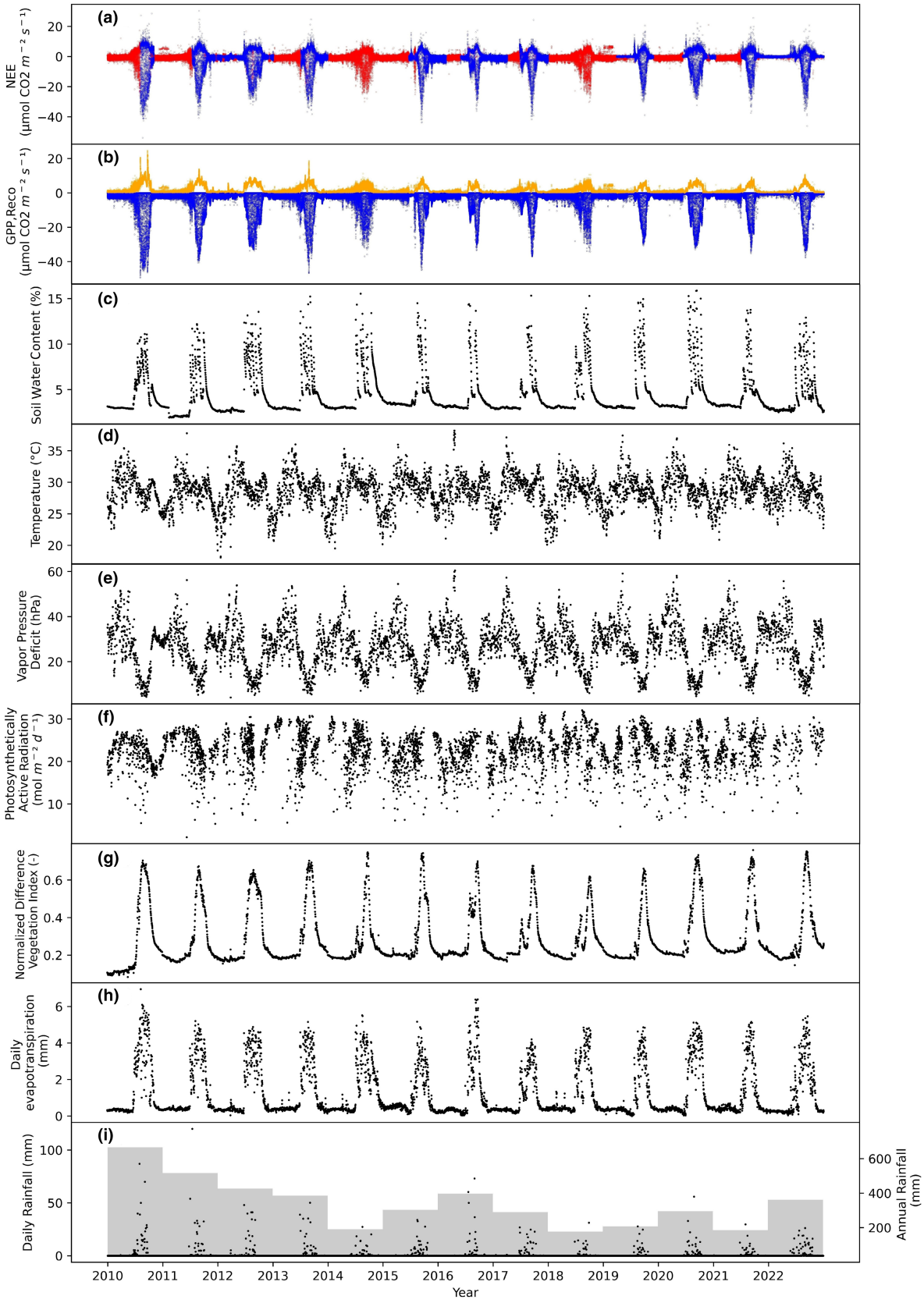

FIGURE 2 The CO_2 exchange fluxes and the environmental variables at the Dahra field site 2010–2022. (a) Half-hourly measured net ecosystem exchange (NEE) (blue) and gap-filled NEE (red); (b) gap-filled half-hourly gross primary production (GPP) (blue) and ecosystem respiration (R_{eco}) (orange); (c) daily mean soil water content, (d) daily mean air temperature (T_{air}), (e) daily mean vapor pressure deficit, (f) daily mean daytime photosynthetically active radiation, (g) daily mean normalized difference vegetation index, (h) daily sums of evapotranspiration (mm), and (i) daily and annual sums of rainfall (points and bars, respectively).

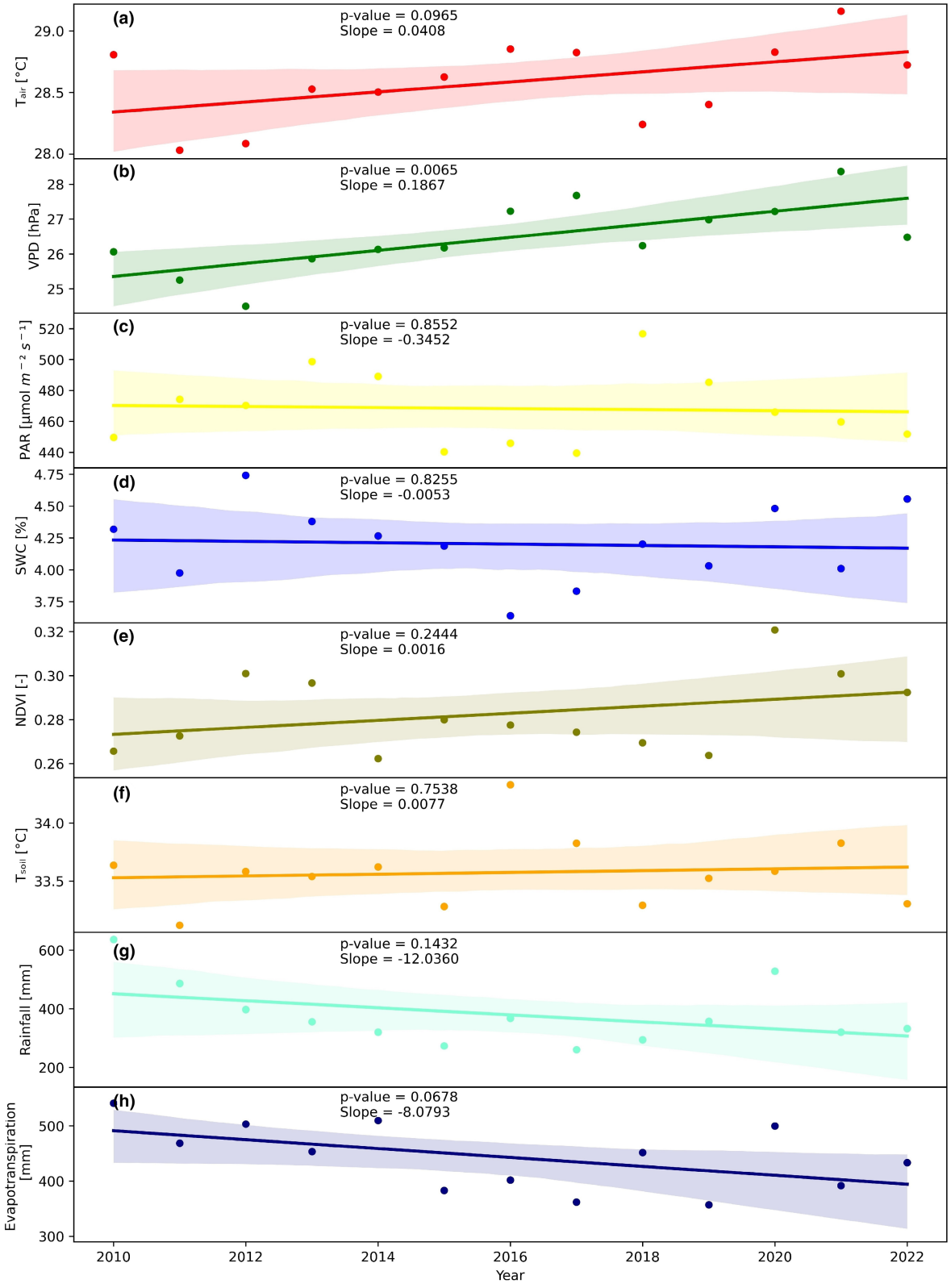

FIGURE 3 Annual environmental variables and their linear trends 2010–2022. Shaded areas show the 95% confidence intervals. (a) Mean air temperature (T_{air}), (b) mean vapor pressure deficit (VPD), (c) mean photosynthetically active radiation (PAR), (d) mean soil water content (SWC), (e) mean normalized difference vegetation index (NDVI), (f) mean soil temperature (T_{soil}), (g) sum of annual rainfall, and (h) sum of annual evapotranspiration.

TABLE 1 Annual and rainy season budgets of net ecosystem exchange (NEE), gross primary production (GPP), and ecosystem respiration (R_{eco}) for the period 2010–2022 with ± total uncertainties. Bottom row depicts average value during the measured period ± budget uncertainty ± standard deviation from interannual variability.

Year	Missing flux data (%)	Annual NEE (g C m^{-2} $year^{-1}$)	Annual GPP (g C m^{-2} $year^{-1}$)	Annual R_{eco} (g C m^{-2} $year^{-1}$)	Rainy season length (days)	Annual sums of rainfall (mm)	Rainy season NEE (g C m^{-2})	Dry season NEE (g C m^{-2})	Rainy season GPP (g C m^{-2})	Dry season GPP (g C m^{-2})	Rainy season R_{eco} (g C m^{-2})	Dry season R_{eco} (g C m^{-2})
2010	89.9	−265 ± 39	−1281 ± 37	1010 ± 36	93	637	−205 ± 31	−61 ± 8	−818 ± 24	−463 ± 13	584 ± 21	427 ± 15
2011	76.0	−215 ± 40	−1051 ± 38	839 ± 37	102	485	−161 ± 30	−55 ± 10	−713 ± 26	−338 ± 12	552 ± 24	288 ± 13
2012	55.1	−182 ± 47	−1059 ± 45	895 ± 44	113	397	−163 ± 42	−19 ± 5	−822 ± 35	−237 ± 10	654 ± 32	240 ± 12
2013	69.2	−236 ± 33	−1018 ± 31	770 ± 29	109	355	−170 ± 23	−66 ± 9	−729 ± 22	−289 ± 9	546 ± 21	223 ± 8
2014	100	−194 ± 16	−842 ± 14	618 ± 10	121	320	−134 ± 11	−60 ± 5	−584 ± 10	−257 ± 4	421 ± 7	197 ± 3
2015	66.5	−232 ± 37	−839 ± 36	572 ± 35	109	273	−149 ± 24	−83 ± 13	−547 ± 23	−293 ± 13	362 ± 22	210 ± 13
2016	51.4	−173 ± 34	−727 ± 33	508 ± 32	94	367	−91 ± 18	−82 ± 16	−452 ± 20	−274 ± 12	318 ± 32	190 ± 12
2017	47.7	−213 ± 34	−809 ± 32	486 ± 31	110	260	−126 ± 20	−86 ± 14	−505 ± 20	−304 ± 12	288 ± 18	199 ± 13
2018	100	−207 ± 16	−803 ± 14	579 ± 10	91	294	−91 ± 7	−115 ± 9	−415 ± 7	−388 ± 7	307 ± 5	273 ± 5
2019	65.4	−97 ± 22	−650 ± 19	480 ± 17	100	357	−68 ± 15	−28 ± 6	−445 ± 13	−205 ± 6	315 ± 11	165 ± 6
2020	67.9	−160 ± 24	−923 ± 21	696 ± 18	107	528	−112 ± 17	−47 ± 7	−620 ± 14	−304 ± 7	468 ± 12	229 ± 6
2021	61.3	−104 ± 22	−683 ± 20	542 ± 17	98	320	−76 ± 16	−28 ± 6	−462 ± 14	−222 ± 6	358 ± 11	185 ± 6
2022	30.2	−57 ± 19	−678 ± 16	591 ± 12	147	332	−86 ± 29	29 ± 10	−591 ± 14	−88 ± 2	481 ± 10	110 ± 2
Avg	67.3 ± 19	−180 ± 29 ± 59	−874 ± 27 ± 178	660 ± 25 ± 163	107 ± 14	379 ± 105	−126 ± 21 ± 41	−54 ± 9 ± 35	−593 ± 9 ± 135	−282 ± 17 ± 87	435 ± 117 ± 121	226 ± 9 ± 73

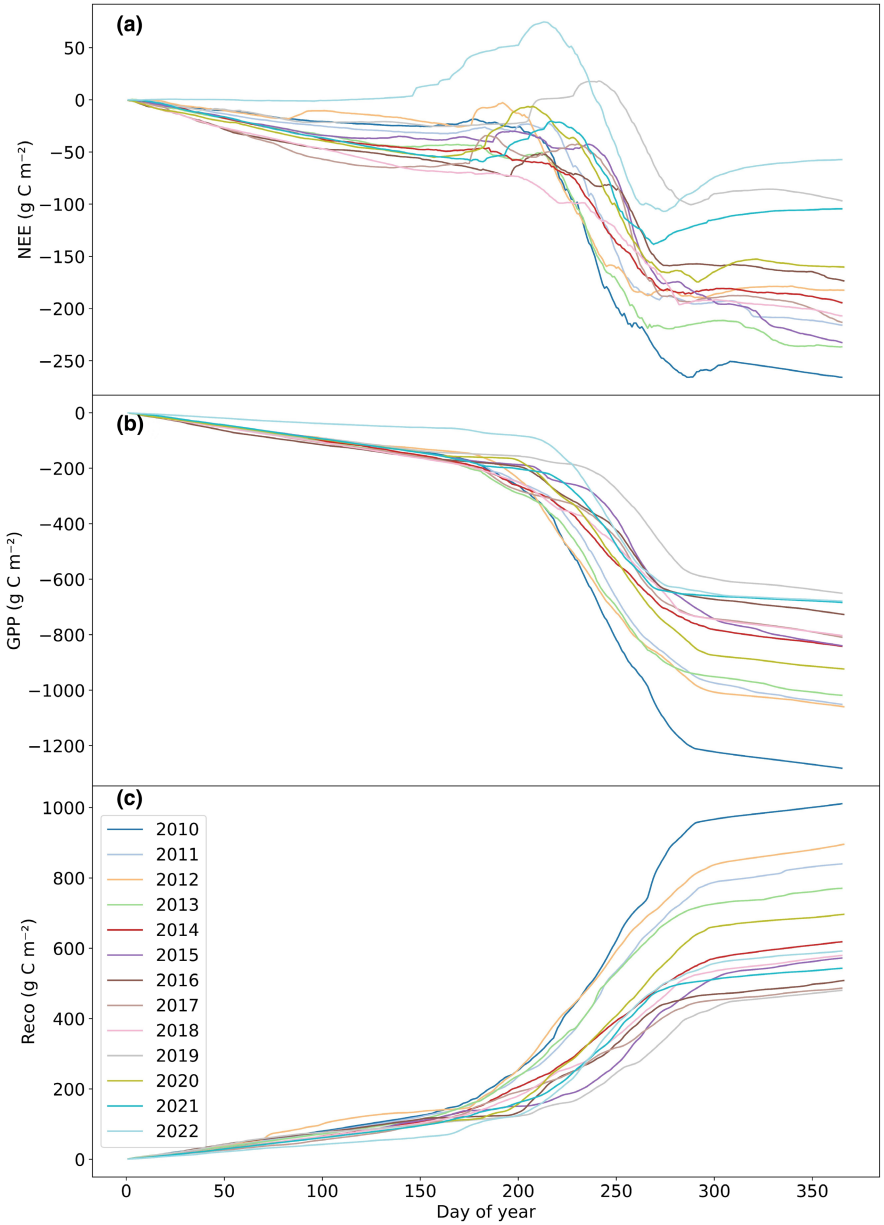

FIGURE 4 Cumulative values of (a) gap-filled net ecosystem exchange (NEE), (b) gross primary production (GPP), and (c) ecosystem respiration (R_{eco}) for the years 2010–2022.

Annual GPP and R_{eco} ranged from −650 ± 19 to −1280 ± 37 g C m^{-2} and 480 ± 17 to 1010 ± 36 g C m^{-2}, respectively (Table 1; Figure 4). The average GPP was −874 ± 27 g C m^{-2} $year^{-1}$ and R_{eco} 660 ± 163 g C m^{-2} $year^{-1}$, with large interannual variation (standard deviation 178 and 163 g C m^{-2} $year^{-1}$ for GPP and R_{eco}, respectively). The R_{eco} and GPP followed a similar seasonal pattern each year, with higher absolute values during the rainy season and lower values during the dry season (Figures 2 and 4).

3.3 | Trends of CO_2 fluxes 2010–2022

Significant trends (±standard error of the fitted trend) over 2010–2022 were found in annual NEE (12.7 ± 2.8 g C $m^{-2}y^{-1}$), GPP (39.6 ± 7.9 g C $m^{-2}y^{-1}$) and R_{eco} budgets (−32 ± 8.9 g C $m^{-2}year^{-1}$) (Figure 5). The NEE trend and the smaller absolute value in the R_{eco} trend compared to the GPP trend indicate a weakening carbon sink that has decreased by 60% during the measuring period (Figure 5). Significant trends were also observed for the rainy and dry season flux budgets, except for the dry season NEE (Figure 5). The absolute levels of the dry season GPP and R_{eco} budget trends were similar across time (~14 g C m^{-2} $year^{-1}$), causing the lack of observed trend for dry season NEE budgets. However, for the rainy season, absolute values of GPP were decreasing more than R_{eco} causing the observed decrease in the annual CO_2 sink.

3.4 | Drivers of the inter-annual variability in the CO_2 flux budgets

The SEM analysis revealed that VPD was the environmental variable most closely related and negatively affecting all GPP and R_{eco} budgets (Figure 6). Rainfall was also important and positively affecting the annual and rainy season budgets. Air temperature positively affected GPP for the rainy and dry season, and R_{eco} for the annual

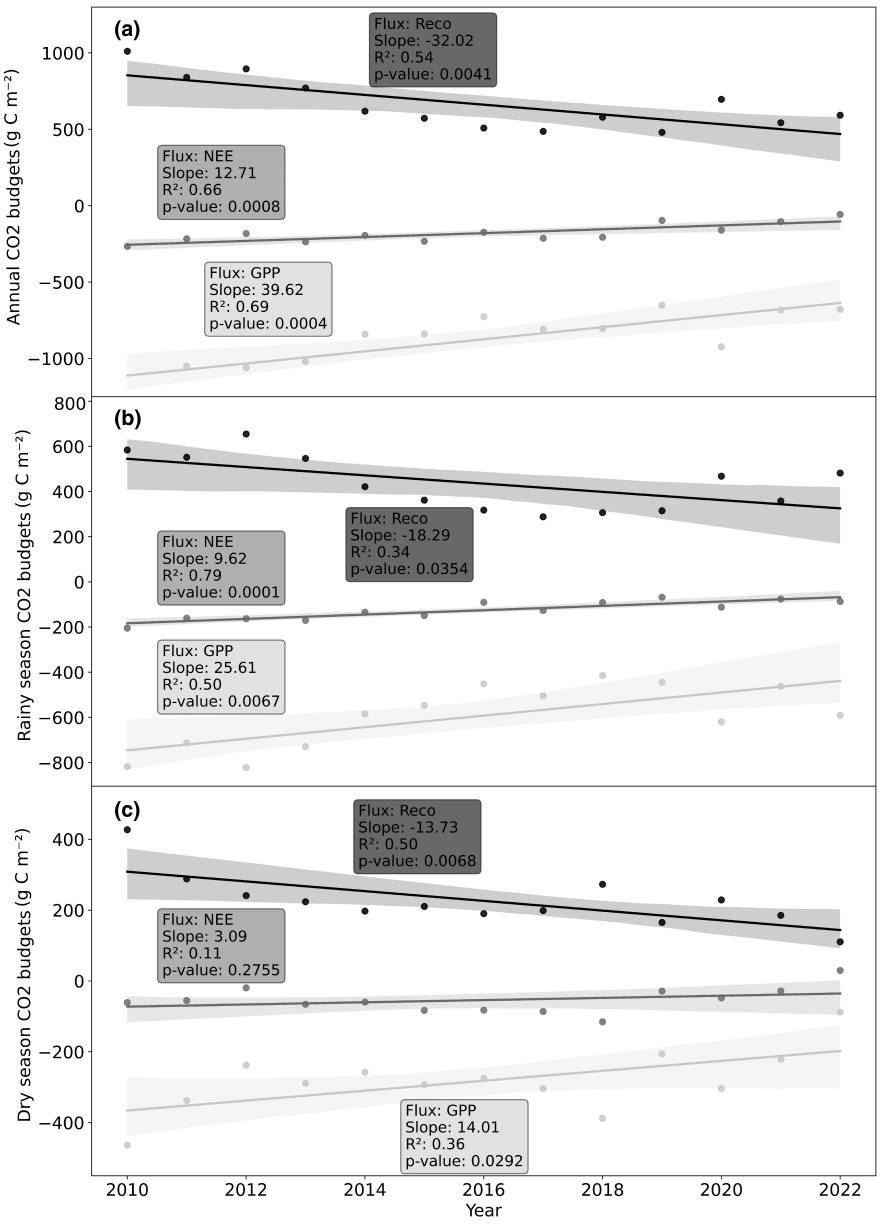

FIGURE 5 Linear trends of annual ($n = 13$) net ecosystem exchange (NEE), gross primary production (GPP) and ecosystem respiration (R_{eco}) at the Dahra field site during 2010–2022 in (a) all year, (b) rainy season, (c) dry season. Shaded areas show 95% confidence intervals.

and dry season budgets. Furthermore, PAR also positively affected annual GPP budgets (Figure 6). No significant effects of SWC on the CO_2 flux budgets were observed. Results of the principal component analysis are provided in the Supporting Information subsection S3.

The annual NEE was not significantly ($p < .05$) correlated with any variable (Table 2). Annual GPP and R_{eco} budgets were correlated with rainfall and VPD (Table 2). For the rainy season, GPP and R_{eco} were correlated with T_{soil}, T_{air}, rainfall, VPD, and SWC. During the dry season, NEE, GPP, and R_{eco} were not correlated with any of the variables (Table 2).

3.5 | Response of WUE and IWUE to changing environmental conditions

Significant trends (±standard error of the fitted trend) were found for annual WUE (-0.051 ± 0.014 g C kg^{-1} H_2O) and IWUE (-0.98 ± 0.42 g C hPa kg^{-1} H_2O) budgets and in the rainy season WUE (-0.055 ± 0.011 g C kg^{-1} H_2O) and IWUE budgets (-0.4 ± 0.18 g C hPa kg^{-1} H_2O). No significant trends were found for the peak of dry season (Figure 7).

4 | DISCUSSION

4.1 | The land–atmosphere CO_2 exchange

The semiarid savanna ecosystem in Dahra, Senegal acted as a carbon sink for all years, but showed a considerable interannual variability (Table 1; Figure 4). Our range of carbon flux budgets were similar to those of other similar semiarid savanna sites in Africa (Ardö et al., 2008; Mougin et al., 2009; Rahimi et al., 2021; Ramier et al., 2009) and on other continents (Mendes et al., 2020; Meza et al., 2018; Scott et al., 2010). The majority of CO_2 exchange took

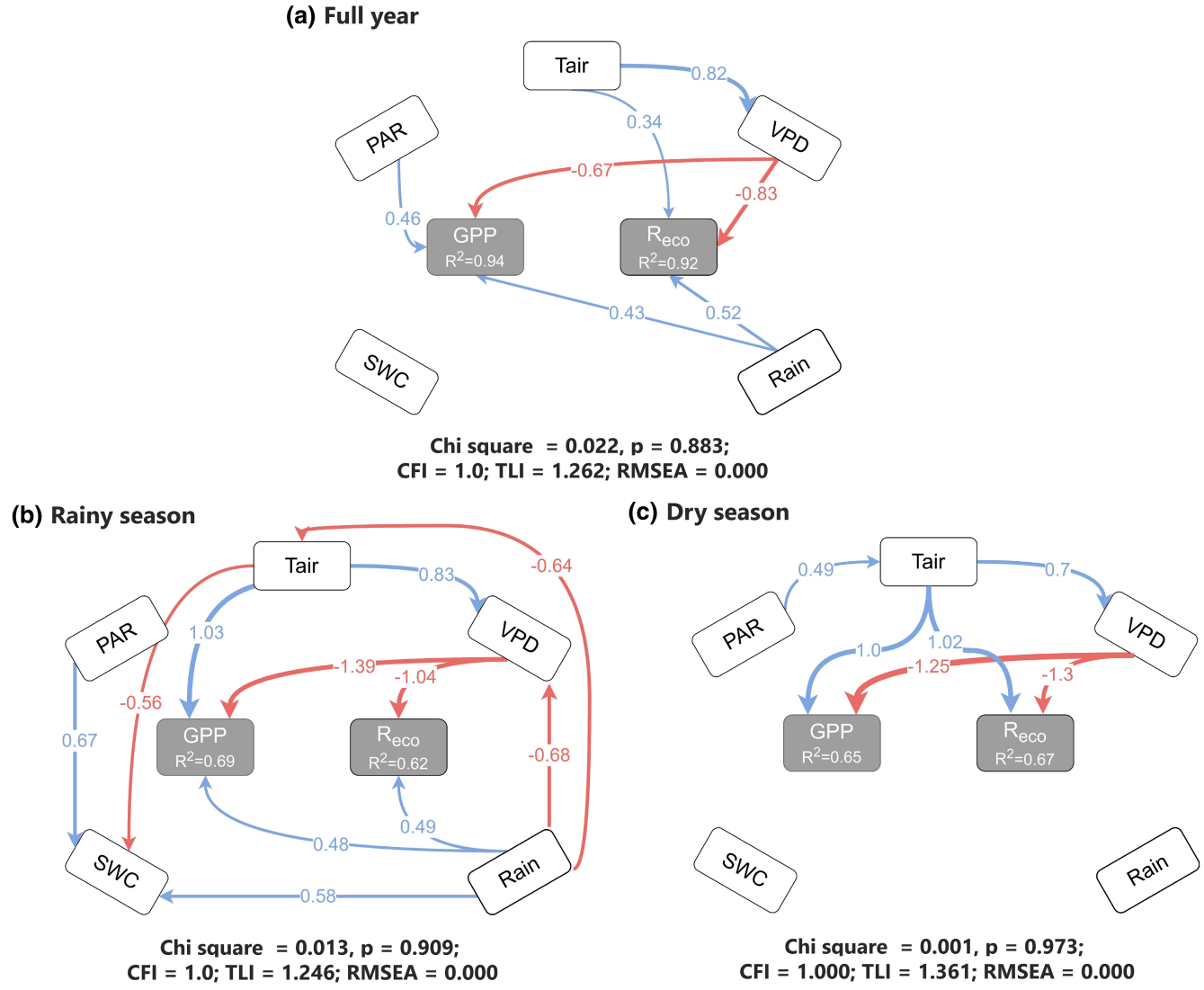

FIGURE 6 Graphical representation of the structural equation model showing the inter-related pathways between environmental variables (photosynthetically active radiation (PAR), vapor pressure deficit (VPD), soil water content (SWC), air temperature (T_{air}), and rainfall (Rain)), and gross primary production (GPP) and ecosystem respiration (R_{eco}) in (a) full year, (b) rainy season, (c) dry season budgets. Values on arrows are standardized path coefficients, representing standardized total effects between variables, line width corresponds to coefficient size. Red and blue lines indicate significantly negative and positive effects ($p < .05$), respectively.

place during the rainy season. The peak of the rainy season showed proportionally higher GPP than R_{eco} (Figures 2 and 4). High GPP at that time can be attributed to abundance of herbaceous C4 plants at the site and their rapid growth during the rainy season (Sibret et al., 2021; Tagesson, Ardö, et al., 2016). During the dry season, the fluxes observed are largely associated with the activity of the trees, as no herbaceous vegetation is present (Figure 1) and microbial activity is inhibited due to the topsoil being dry (Agbohessou et al., 2023). The C3 trees found in this Sahelian semiarid savanna, such as *Balanites aegyptica* (Hall & Walker, 1991; Rojas-Sandoval, 2016) and *Vachellia tortilis*, are adapted to prolonged dry periods due to exceptionally deep root systems (>25 m) (Belsky, 1994; Do et al., 2008; Roupsard et al., 1999; Stone & Kalisz, 1991) and are thus able to maintain their physiological functions, including photosynthesis and respiration. A study by Roupsard et al. (1999) demonstrated that the Sahelian trees, similar to the ones on our site, are able to efficiently utilize groundwater during the dry season. In a synthesis study of six Eddy towers across the Sahel (Tagesson, Fensholt, et al., 2016), a dry season uptake was shown at all of those sites (mean GPP: -0.52 ± 0.15 g C m^{-2} day^{-1}).

Due to the technical issues, there were nine data gaps longer than 50 days during the measuring period, including the full years of 2014 and 2018. We used an RF algorithm for gap-filling as it has been found to outperform other machine learning-based algorithms to fill long gaps in EC data (Irvin et al., 2021; Kim et al., 2020; Mahabbati et al., 2021; Yao et al., 2021; Zhu et al., 2022). Considering these findings and a good performance of RF gap filling (Supporting Information subsection S2), we consider the annual budgets to be reliable despite the long data gaps. Nevertheless, the majority of the CO_2 exchange is occurring during the rainy season of which 51% of

Variable	Season	NEE	GPP	R_{eco}
VPD	Annual	.41	.63*	−.69**
	Rainy	.53	.76**	−.78**
	Dry	.41	.38	−.39
T_{air}	Annual	.24	.3	−.35
	Rainy	.29	.58*	−.66*
	Dry	.11	.02	−.05
T_{soil}	Annual	.06	.21	−.28
	Rainy	.46	.72**	−.83***
	Dry	.06	−.23	.28
PAR	Annual	−.06	−.02	.07
	Rainy	−.13	−.11	.16
	Dry	−.07	−.02	.11
SWC	Annual	.07	−.38	.54
	Rainy	−.4	−.62*	.68*
	Dry	−.3	−.17	.2
Rainfall	Annual	−.5	−.81***	.82***
	Rainy	−.66*	−.75**	.7*
Rainy season length	Annual	.39	.14	−.01
NDVI sum	Annual	.29	−.18	.36
	Rainy	−.45	−.33	.4
Peak NDVI	Annual	.28	.16	−.09

*$p < .050$. **$p < .01$. ***$p < .001$.

TABLE 2 Correlation coefficients between interannual and inter-seasonal variability in average values of environmental variables (sums for rainfall) and the averages of the net ecosystem exchange (NEE), gross primary production (GPP), and ecosystem respiration (R_{eco}) ($n = 13$). The environmental variables are vapor pressure deficit (VPD) (hPa), air temperature (T_{air}) (°C), soil temperature (T_{soil}) (°C), photosynthetically active radiation (PAR) ($\mu mol\, m^{-2}\, s^{-1}$), soil water content measured at 5 cm depth (SWC) (%), rainfall (mm), rainy season length, normalized difference vegetation index (NDVI) (-). For NDVI, the correlations are taken both for the sums of the annual and rainy season budgets and for the annual peak values.

the time series was captured. This is a similar rate to other EC flux studies (Jensen et al., 2017; López-Blanco et al., 2017; Tagesson, Fensholt, et al., 2016), and similar to as what can be seen in Fluxnet (Baldocchi et al., 2001).

Another possible source of uncertainty is the swap of analyzer from the open-path LI-7500 to the closed-path CPEC200 system. However, several studies have shown a close linear relationship for CO_2 fluxes measured between these two analyzers (Kang et al., 2019; Novick et al., 2013; Polonik et al., 2019). Additionally, no clear breakpoint can be seen in the budget trends prior and post the analyzer change (before and after 2018 in Figure 5), and we thus conclude that this sensor replacement did not change the outcome of the measured trends.

4.2 | Interannual trends of CO_2 fluxes and its drivers

The observed decreasing carbon sink of this semiarid savanna ecosystem is in contrast with numerous studies that shows increasing sink strength in semiarid regions globally (Friedlingstein et al., 2023; Hutley et al., 2022; Ross et al., 2021; Ruehr et al., 2023; Sitch et al., 2015). These studies suggest that the increasing carbon sink is caused by CO_2 fertilization. Instead, we observed an increase in atmospheric dryness (VPD) but no trend in neither SWC nor rainfall (Figure 3), and that VPD is likely the most important variable driving the trends of GPP and R_{eco}, and thus NEE (Figure 6). Thus, despite no change in soil water availability, a strong decreasing trend was observed. Atmospheric dryness (VPD) is known to be one of the most important limiting factors of plant growth and therefore carbon sequestration (Abdi et al., 2017; Grossiord et al., 2020; Kannenberg et al., 2024; Liu et al., 2023; Novick et al., 2024; Zhong et al., 2023). Increasing VPD causes stomatal closure, decreasing the potential increase of carbon uptake due to CO_2 fertilization (Li et al., 2023). Thus, for conditions of continued atmospheric drying, the carbon sink may still be decreasing despite sufficient water availability and increasing atmospheric CO_2 levels (Ru et al., 2022; Song et al., 2024; Yang et al., 2021). Future projections of the Western part of Sahel indicate that rainfall will decrease and temperature will increase, respectively, suggesting an increase in VPD (Biasutti, 2019; Trisos et al., 2022; Lavaysse et al., 2010). Hence, if these projections are accurate, our results suggest a continued decrease in net CO_2 uptake. It is therefore of high importance to measure ongoing environmental changes across the Sahel, and their implications on ecosystem functioning and services.

The range of WUE from 1.5 to 4 g C kg^{-1} H_2O is similar to other semiarid regions (Tang et al., 2014; Xue et al., 2015). It is known that WUE decreases with drought in semiarid ecosystems, as GPP decreases more than ET during dry years (Yang et al., 2016). Negative trends were indeed seen for the rainy season (Figure 7). The main reason is probably the sufficient amount of water for evaporation, as indicated by the stable trends in SWC and rainfall, and the increasing trend in VPD having a stronger effect on the GPP than on the transpiration. Another cause of the negative rainy season WUE trends

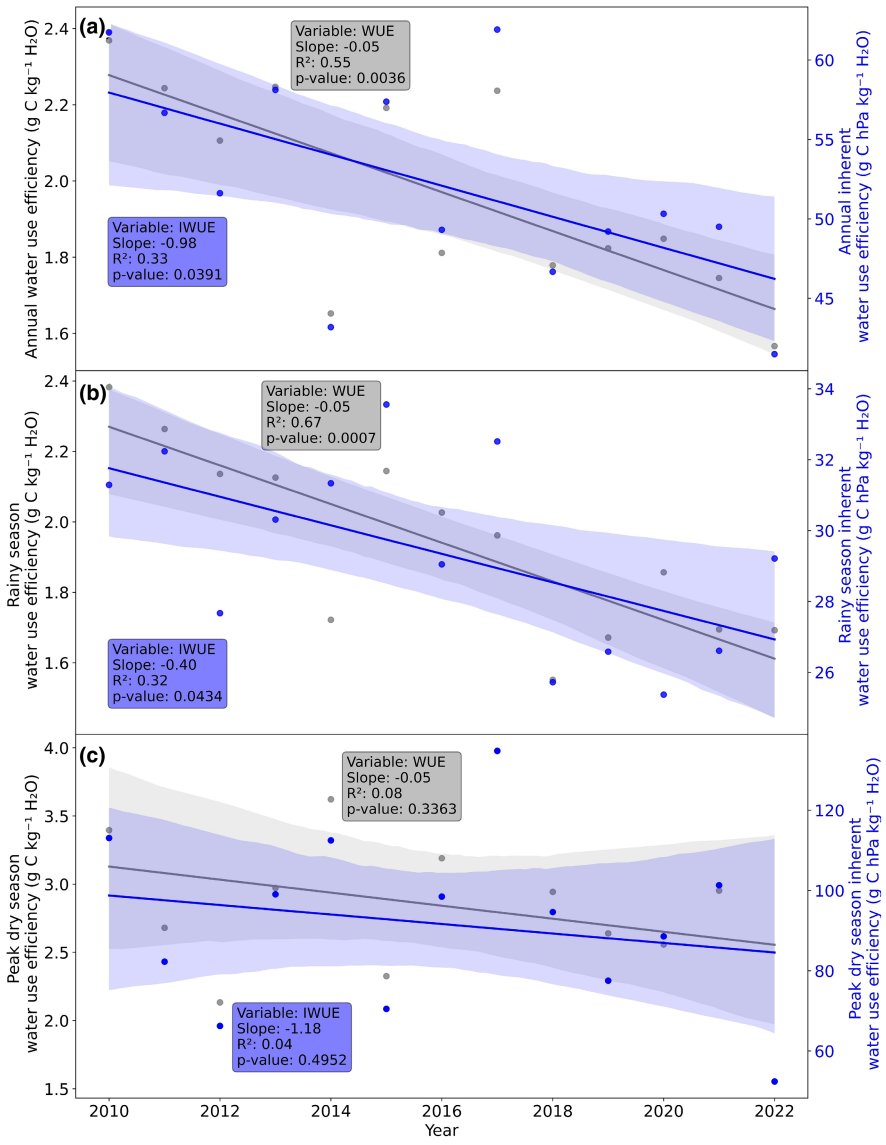

FIGURE 7 Linear trends of annual ($n = 13$) water use efficiency (WUE), inherent water use efficiency 2010–2022 in (a) all year, (b) rainy season, (c) peak of dry season. Shaded areas show the 95% confidence intervals.

could be a shift in herbaceous species composition (see paragraph below) (De Boeck et al., 2006; Gebremedhn et al., 2023). However, we found no trends in the end of the dry season WUE and IWUE, indicating that trends in both GPP and ET are negatively affected in a similar manner. During the end of the dry season, ET mainly comes the transpiration of the trees (trees being the only active vegetation during this part of the year, and no loss of water from the soil surface as seen in the stable SWC). The stable WUE of trees can be explained by effective regulation of the tree canopy conductance (Barron-Gafford et al., 2012; Niziński et al., 2019). The trees thereby decrease stomatal conductance with the increased VPD, negatively affecting both GPP and ET. The most prevalent tree species at our site have indeed previously been found to have stable WUE in both dry and moist years (Gebrekirstos et al., 2011). Another possible reason for the divergent responses of the rainy and dry seasons WUE is increasing atmospheric CO_2 concentration, which has a more positive effect on GPP of C3 trees than of the C4 grasses (Chen et al., 2022).

The lack of correlation between interannual R_{eco} and GPP versus NDVI surprisingly indicates that the decrease in CO_2 fluxes may be decoupled from the vegetation greenness (Table 2). We found no significant trends of NDVI on the site (Figure 3). The discrepancy between NDVI and the CO_2 flux trends could be explained by the effect of grazing and herbaceous species composition. Gebremedhn et al. (2023) have shown that the area within the proximity of the tower is intensely grazed and that the most prevalent species attributed to high grazing is *Zornia glochidiata*. This particular species is a planophile (i.e., leaves arranged in horizontal plane), and Mbow et al. (2013) found that this species is characterized by high peak NDVI yet with low biomass accumulation. Thus, intensified grazing could be leading to a shift in species composition (increased contribution of *Zornia glochidiata*) positively affecting NDVI, but with low productivity of biomass (i.e., low GPP).

The findings of Jiang et al. (2022) and Zeng et al. (2023) indicate that despite an overall greening trend of the Sahel during 2001–2020, some regions in the western part experienced a browning trend throughout that period. Thus, considering the heterogeneity of the Sahel, the observed changes in carbon sink strength might vary across the region. The decreasing carbon sink strength and its

relationship with changing environmental conditions showcases that semiarid ecosystems will be severely affected by climate change. The projected warmer climate coupled with decreasing rainfall may lead to an increase in atmospheric dryness, which may lead to decreased GPP across this biome, and thus lower carbon sequestration rates. Long-term observations of climate–carbon cycle interactions are pivotal for understanding these interactions and assess the rate of change of ecosystem functions and services. Considering that the semiarid regions dominate the trend and the interannual variability of global carbon sink (Ahlström et al., 2015) and that the Sahel is one of the largest semiarid regions in the world, the results of this study are valuable for assessing impact these changes may have on the global carbon cycle dynamics.

AUTHOR CONTRIBUTIONS

Aleksander Wieckowski: Conceptualization; data curation; formal analysis; investigation; methodology; software; validation; visualization; writing – original draft; writing – review and editing. **Patrik Vestin:** Conceptualization; methodology; supervision; writing – review and editing. **Jonas Ardö:** Conceptualization; methodology; supervision; writing – review and editing. **Olivier Roupsard:** Writing – review and editing. **Ousmane Ndiaye:** Writing – review and editing. **Ousmane Diatta:** Writing – review and editing. **Seydina Ba:** Writing – review and editing. **Yélognissè Agbohessou:** Writing – review and editing. **Rasmus Fensholt:** Writing – review and editing. **Wim Verbruggen:** Writing – review and editing. **Haftay Hailu Gebremedhn:** Writing – review and editing. **Torbern Tagesson:** Conceptualization; data curation; funding acquisition; investigation; methodology; project administration; resources; supervision; writing – review and editing.

ACKNOWLEDGEMENTS

This project was funded by FORMAS (Dnr 2021-00644) and the Carbon Sequestration and Green-house Gas Emissions in (Agro) Sylvopastoral Ecosystems in the Sahelian CILSS States (CaSSECS) project, supported by the European Union under the Development Smart Innovation through Research in Agriculture (DeSIRA) Initiative (FOOD/2019/410-169). Torbern Tagesson also acknowledges funding from the Swedish National Space Agency (SNSA Dnr 2021-00144; 2021-00111), FORMAS (Dnr 2023-02436), and Carl Tryggers Stiftelse. Wim Verbruggen was funded by VILLUM FONDEN in the framework of the DRYTIP (Drought-induced tipping points in ecosystem functioning) project (Grant. 37465). Rasmus Fensholt acknowledges funding from the Independent Research Fund Denmark, Unravelling climate change impacts on savanna vegetation ecosystems (CLISA), grant ID: 10.46540/2032-00026B. Ardö acknowledges funding from Lund University through an infrastructure grant (Dnr 2012/377). The research presented in this paper is a contribution to the Strategic Research Area "Biodiversity and Ecosystem Services in a Changing Climate," BECC, funded by the Swedish Government. We are very grateful to the Institut Sénégalais de Recherche Agricole for all logistic, administrative, and technical support. Thanks also to our guards who provided night and day surveillance of the study site.

CONFLICT OF INTEREST STATEMENT

The authors declare no conflicts of interest.

DATA AVAILABILITY STATEMENT

The data that support the findings of this study are openly available on Dryad at: https://doi.org/10.5061/dryad.3ffbg79t0.

ORCID

Aleksander Wieckowski https://orcid.org/0000-0003-1544-9794
Yélognissè Agbohessou https://orcid.org/0000-0002-2681-0162
Wim Verbruggen https://orcid.org/0000-0002-3611-6561

REFERENCES

Abdi, A., Seaquist, J., Tenenbaum, D., Eklundh, L., & Ardö, J. (2014). The supply and demand of net primary production in the Sahel. *Environmental Research Letters*, *9*(9), 094003. https://doi.org/10.1088/1748-9326/9/9/094003

Abdi, A. M., Boke-Olén, N., Tenenbaum, D. E., Tagesson, T., Cappelaere, B., & Ardö, J. (2017). Evaluating water controls on vegetation growth in the semi-arid Sahel using field and earth observation data. *Remote Sensing*, *9*(3), 294. https://doi.org/10.3390/rs9030294

Adaawen, S., Rademacher-Schulz, C., Schraven, B., & Segadlo, N. (2019). Drought, migration, and conflict in sub-Saharan Africa: What are the links and policy options? *Current Directions in Water Scarcity Research*, *2*, 15–31. https://doi.org/10.1016/B978-0-12-814820-4.00002-X

Agbohessou, Y., Delon, C., Mougin, E., Grippa, M., Tagesson, T., Diedhiou, M., Ba, S., Ngom, D., Vezy, R., Ndiaye, O., Assouma, M. H., Diawara, M., & Roupsard, O. (2023). To what extent are greenhouse-gas emissions offset by trees in a Sahelian silvopastoral system? *Agricultural and Forest Meteorology*, *343*, 109780. https://doi.org/10.1016/j.agrformet.2023.109780

Ahlström, A., Raupach, M. R., Schurgers, G., Smith, B., Arneth, A., Jung, M., Reichstein, M., Canadell, J. G., Friedlingstein, P., & Jain, A. K. (2015). The dominant role of semi-arid ecosystems in the trend and variability of the land CO_2 sink. *Science*, *348*(6237), 895–899.

Ardö, J., Mölder, M., El-Tahir, B. A., & Elkhidir, H. A. M. (2008). Seasonal variation of carbon fluxes in a sparse savanna in semi arid Sudan. *Carbon Balance and Management*, *3*, 1–18. https://doi.org/10.1186/1750-0680-3-7

Baldocchi, D., Falge, E., Gu, L., Olson, R., Hollinger, D., Running, S., Anthoni, P., Bernhofer, C., Davis, K., & Evans, R. (2001). FLUXNET: A new tool to study the temporal and spatial variability of ecosystem-scale carbon dioxide, water vapor, and energy flux densities. *Bulletin of the American Meteorological Society*, *82*(11), 2415–2434. https://doi.org/10.1175/1520-0477(2001)082<2415:FANTTS>2.3.CO;2

Barron-Gafford, G. A., Scott, R. L., Jenerette, G. D., Hamerlynck, E. P., & Huxman, T. E. (2012). Temperature and precipitation controls over leaf-and ecosystem-level CO_2 flux along a woody plant encroachment gradient. *Global Change Biology*, *18*(4), 1389–1400. https://doi.org/10.1111/j.1365-2486.2011.02599.x

Beer, C., Ciais, P., Reichstein, M., Baldocchi, D., Law, B. E., Papale, D., Soussana, J. F., Ammann, C., Buchmann, N., & Frank, D. (2009). Temporal and among-site variability of inherent water use efficiency at the ecosystem level. *Global Biogeochemical Cycles*, *23*(2), GB2018. https://doi.org/10.1029/2008GB003233

Belsky, A. J. (1994). Influences of trees on savanna productivity: Tests of shade, nutrients, and tree-grass competition. *Ecology*, *75*(4), 922–932. https://doi.org/10.2307/1939416

Biasutti, M. (2019). Rainfall trends in the African Sahel: Characteristics, processes, and causes. *Wiley Interdisciplinary Reviews: Climate Change*, *10*(4), e591. https://doi.org/10.1002/wcc.591

Booker, K., Huntsinger, L., Bartolome, J. W., Sayre, N. F., & Stewart, W. (2013). What can ecological science tell us about opportunities for carbon sequestration on arid rangelands in the United States? *Global Environmental Change*, *23*(1), 240–251. https://doi.org/10.1016/j.gloenvcha.2012.10.001

Boulain, N., Cappelaere, B., Ramier, D., Issoufou, H., Halilou, O., Seghieri, J., Guillemin, F., Oi, M., Gignoux, J., & Timouk, F. (2009). Towards an understanding of coupled physical and biological processes in the cultivated Sahel–2. Vegetation and carbon dynamics. *Journal of Hydrology*, *375*(1–2), 190–203. https://doi.org/10.1016/j.jhydrol.2008.11.045

Breiman, L. (2001). Random forests. *Machine Learning*, *45*, 5–32. https://doi.org/10.1023/A:1010933404324

Chen, C., Riley, W. J., Prentice, I. C., & Keenan, T. F. (2022). CO_2 fertilization of terrestrial photosynthesis inferred from site to global scales. *Proceedings of the National Academy of Sciences of the United States of America*, *119*(10), e2115627119. https://doi.org/10.1073/pnas.2115627119

De Boeck, H., Lemmens, C., Bossuyt, H., Malchair, S., Carnol, M., Merckx, R., Nijs, I., & Ceulemans, R. (2006). How do climate warming and plant species richness affect water use in experimental grasslands? *Plant and Soil*, *288*, 249–261. https://doi.org/10.1007/s11104-006-9112-5

Ding, R., Kang, S., Li, F., Zhang, Y., Tong, L., & Sun, Q. (2010). Evaluating eddy covariance method by large-scale weighing lysimeter in a maize field of northwest China. *Agricultural Water Management*, *98*(1), 87–95. https://doi.org/10.1016/j.agwat.2010.08.001

Ding, Z., Wang, Y., Ding, J., Ren, Z., & Liao, J. (2024). Dynamics of carbon and water vapor fluxes in three typical ecosystems of Heihe River Basin, Northwestern China. *Science of the Total Environment*, *929*, 172611. https://doi.org/10.1016/j.scitotenv.2024.172611

Do, F. C., Rocheteau, A., Diagne, A. L., Goudiaby, V., Granier, A., & Lhomme, J.-P. (2008). Stable annual pattern of water use by *Acacia tortilis* in Sahelian Africa. *Tree Physiology*, *28*(1), 95–104. https://doi.org/10.1093/treephys/28.1.95

Fan, S. M., Wofsy, S. C., Bakwin, P. S., Jacob, D. J., & Fitzjarrald, D. R. (1990). Atmosphere-biosphere exchange of CO_2 and O_3 in the central Amazon forest. *Journal of Geophysical Research: Atmospheres*, *95*(D10), 16851–16864. https://doi.org/10.1029/JD095iD10p16851

Fan, Y., Chen, J., Shirkey, G., John, R., Wu, S. R., Park, H., & Shao, C. (2016). Applications of structural equation modeling (SEM) in ecological studies: An updated review. *Ecological Processes*, *5*, 1–12. https://doi.org/10.1186/s13717-016-0063-3

Finkelstein, P. L., & Sims, P. F. (2001). Sampling error in eddy correlation flux measurements. *Journal of Geophysical Research: Atmospheres*, *106*(D4), 3503–3509. https://doi.org/10.1029/2000JD900731

Flores-Rentería, D., Delgado-Balbuena, J., Campuzano, E. F., & Yuste, J. C. (2023). Seasonal controlling factors of CO_2 exchange in a semi-arid shrubland in the Chihuahuan Desert, Mexico. *Science of the Total Environment*, *858*, 159918. https://doi.org/10.1016/j.scitotenv.2022.159918

Foken, T., Göckede, M., Mauder, M., Mahrt, L., Amiro, B., & Munger, J. W. (2004). Post-field data quality control. In *Handbook of micrometeorology: A guide for surface flux measurement and analysis* (Vol. *29*, pp. 181–208). Springer. https://doi.org/10.1007/1-4020-2265-4_9

Friedlingstein, P., O'sullivan, M., Jones, M. W., Andrew, R. M., Bakker, D. C., Hauck, J., Landschützer, P., Le Quéré, C., Luijkx, I. T., & Peters, G. P. (2023). Global Carbon Budget 2023. *Earth System Science Data*, *15*(12), 5301–5369. https://doi.org/10.5194/essd-15-5301-2023

Gamon, J. A., Coburn, C., Flanagan, L. B., Huemmrich, K. F., Kiddle, C., Sanchez-Azofeifa, G. A., Thayer, D. R., Vescovo, L., Gianelle, D., Sims, D. A., Rahman, A. F., & Pastorello, G. Z. (2010). SpecNet revisited: Bridging flux and remote sensing communities. *Canadian Journal of Remote Sensing*, *36*(Suppl. 2), S376–S390. https://doi.org/10.5589/m10-067

Gebrekirstos, A., van Noordwijk, M., Neufeldt, H., & Mitlöhner, R. (2011). Relationships of stable carbon isotopes, plant water potential and growth: An approach to asses water use efficiency and growth strategies of dry land agroforestry species. *Trees*, *25*, 95–102. https://doi.org/10.1007/s00468-010-0467-0

Gebremedhn, H. H., Ndiaye, O., Mensah, S., Fassinou, C., Taugourdeau, S., Tagesson, T., & Salgado, P. (2023). Grazing effects on vegetation dynamics in the savannah ecosystems of the Sahel. *Ecological Processes*, *12*(1), 54. https://doi.org/10.1186/s13717-023-00468-3

Grace, J. B., & Bollen, K. A. (2005). Interpreting the results from multiple regression and structural equation models. *Bulletin of the Ecological Society of America*, *86*(4), 283–295. https://doi.org/10.1890/0012-9623(2005)86[283:itrfmr]2.0.co;2

Grossiord, C., Buckley, T. N., Cernusak, L. A., Novick, K. A., Poulter, B., Siegwolf, R. T., Sperry, J. S., & McDowell, N. G. (2020). Plant responses to rising vapor pressure deficit. *New Phytologist*, *226*(6), 1550–1566. https://doi.org/10.1111/nph.16485

Grossiord, C., Sevanto, S., Borrego, I., Chan, A. M., Collins, A. D., Dickman, L. T., Hudson, P. J., McBranch, N., Michaletz, S. T., & Pockman, W. T. (2017). Tree water dynamics in a drying and warming world. *Plant, Cell & Environment*, *40*(9), 1861–1873. https://doi.org/10.1111/pce.12991

Gu, Q., Wei, J., Luo, S., Ma, M., & Tang, X. (2018). Potential and environmental control of carbon sequestration in major ecosystems across arid and semi-arid regions in China. *Science of the Total Environment*, *645*, 796–805. https://doi.org/10.1016/j.scitotenv.2018.07.139

Hall, J., & Walker, D. (1991). *B. aegyptiaca—A monograph*. School of Agricultural and Forest Science, University of Wales.

Hanan, N., Elbers, J., Kabat, P., Dolman, A., & De Bruin, H. (1996). CO2 flux and photosynthesis of a Sahelian savanna during HAPEX-Sahel. *Physics and Chemistry of the Earth*, *21*(3), 135–141. https://doi.org/10.1016/S0079-1946(97)85574-7

Hickler, T., Eklundh, L., Seaquist, J. W., Smith, B., Ardö, J., Olsson, L., Sykes, M. T., & Sjöström, M. (2005). Precipitation controls Sahel greening trend. *Geophysical Research Letters*, *32*(21), L21415. https://doi.org/10.1029/2005GL024370

Hutley, L. B., Beringer, J., Fatichi, S., Schymanski, S. J., & Northwood, M. (2022). Gross primary productivity and water use efficiency are increasing in a high rainfall tropical savanna. *Global Change Biology*, *28*(7), 2360–2380. https://doi.org/10.1111/gcb.16012

Irvin, J., Zhou, S., McNicol, G., Lu, F., Liu, V., Fluet-Chouinard, E., Ouyang, Z., Knox, S. H., Lucas-Moffat, A., & Trotta, C. (2021). Gap-filling eddy covariance methane fluxes: Comparison of machine learning model predictions and uncertainties at FLUXNET-CH4 wetlands. *Agricultural and Forest Meteorology*, *308*, 108528. https://doi.org/10.1016/j.agrformet.2021.108528

Jensen, R., Herbst, M., & Friborg, T. (2017). Direct and indirect controls of the interannual variability in atmospheric CO_2 exchange of three contrasting ecosystems in Denmark. *Agricultural and Forest Meteorology*, *233*, 12–31. https://doi.org/10.1016/j.agrformet.2016.10.023

Jiang, M., Jia, L., Menenti, M., & Zeng, Y. (2022). Understanding spatial patterns in the drivers of greenness trends in the Sahel-Sudano-Guinean region. *Big Earth Data*, *1-20*, 298–317. https://doi.org/10.1080/20964471.2022.2146632

Kang, M., Kim, J., Yang, H., Lim, J.-H., Chun, J.-H., & Moon, M. (2019). On securing continuity of long-term observational eddy flux data: Field intercomparison between open-and enclosed-path gas analyzers. *Korean Journal of Agricultural and Forest Meteorology*, *21*(3), 135–145. https://doi.org/10.5532/KJAFM.2019.21.3.135

Kannenberg, S. A., Anderegg, W. R., Barnes, M. L., Dannenberg, M. P., & Knapp, A. K. (2024). Dominant role of soil moisture in mediating carbon and water fluxes in dryland ecosystems. *Nature Geoscience*, *17*, 38–43. https://doi.org/10.1038/s41561-023-01351-8

Kattge, J., Bönisch, G., Díaz, S., Lavorel, S., Prentice, I. C., Leadley, P., Tautenhahn, S., Werner, G. D. A., Aakala, T., Abedi, M., Acosta, A. T. R., Adamidis, G. C., Adamson, K., Aiba, M., Albert, C. H., Alcántara, J. M., Alcázar, C., Aleixo, I., Ali, H., … Wirth, C. (2020). TRY plant trait database—Enhanced coverage and open access. *Global Change Biology*, *26*(1), 119–188. https://doi.org/10.1111/gcb.14904

Kim, Y., Johnson, M. S., Knox, S. H., Black, T. A., Dalmagro, H. J., Kang, M., Kim, J., & Baldocchi, D. (2020). Gap-filling approaches for eddy covariance methane fluxes: A comparison of three machine learning algorithms and a traditional method with principal component analysis. *Global Change Biology*, *26*(3), 1499–1518. https://doi.org/10.1111/gcb.14845

Lasslop, G., Reichstein, M., Papale, D., Richardson, A. D., Arneth, A., Barr, A., Stoy, P., & Wohlfahrt, G. (2010). Separation of net ecosystem exchange into assimilation and respiration using a light response curve approach: Critical issues and global evaluation. *Global Change Biology*, *16*(1), 187–208. https://doi.org/10.1111/j.1365-2486.2009.02041.x

Lavaysse, C., Flamant, C., & Janicot, S. (2010). Regional-scale convection patterns during strong and weak phases of the Saharan heat low. *Atmospheric Science Letters*, *11*(4), 255–264. https://doi.org/10.1002/asl.284

Li, S., Wang, G., Zhu, C., Lu, J., Ullah, W., Hagan, D. F. T., Kattel, G., Liu, Y., Zhang, Z., & Song, Y. (2023). Vegetation growth due to CO_2 fertilization is threatened by increasing vapor pressure deficit. *Journal of Hydrology*, *619*, 129292. https://doi.org/10.1016/j.jhydrol.2023.129292

Liu, X., Sun, G., Fu, Z., Ciais, P., Feng, X., Li, J., & Fu, B. (2023). Compound droughts slow down the greening of the Earth. *Global Change Biology*, *29*(11), 3072–3084. https://doi.org/10.1111/gcb.16657

López-Blanco, E., Lund, M., Williams, M., Tamstorf, M. P., Westergaard-Nielsen, A., Exbrayat, J.-F., Hansen, B. U., & Christensen, T. R. (2017). Exchange of CO_2 in Arctic tundra: Impacts of meteorological variations and biological disturbance. *Biogeosciences*, *14*(19), 4467–4483. https://doi.org/10.5194/bg-14-4467-2017

Ma, L., Qiao, C., Du, L., Tang, E., Wu, H., Shi, G., Xue, B., Wang, Y., & Lucas-Borja, M. E. (2024). Drought in the middle growing season inhibited carbon uptake more critical in an anthropogenic shrub ecosystem of Northwest China. *Agricultural and Forest Meteorology*, *353*, 110060. https://doi.org/10.1016/j.agrformet.2024.110060

Mahabbati, A., Beringer, J., Leopold, M., McHugh, I., Cleverly, J., Isaac, P., & Izady, A. (2021). A comparison of gap-filling algorithms for eddy covariance fluxes and their drivers. *Geoscientific Instrumentation, Methods and Data Systems*, *10*(1), 123–140. https://doi.org/10.5194/gi-10-123-2021

Mauder, M., Foken, T., Aubinet, M., & Ibrom, A. (2021). Eddy-covariance measurements. In T. Foken (Ed.), *Springer handbook of atmospheric measurements* (pp. 1473–1504). Springer Handbooks, Springer. https://doi.org/10.1007/978-3-030-52171-4_55

Mbow, C., Fensholt, R., Rasmussen, K., & Diop, D. (2013). Can vegetation productivity be derived from greenness in a semi-arid environment? Evidence from ground-based measurements. *Journal of Arid Environments*, *97*, 56–65. https://doi.org/10.1016/j.jaridenv.2013.05.011

Mendes, K. R., Campos, S., da Silva, L. L., Mutti, P. R., Ferreira, R. R., Medeiros, S. S., Perez-Marin, A. M., Marques, T. V., Ramos, T. M., & de Lima Vieira, M. M. (2020). Seasonal variation in net ecosystem CO_2 exchange of a Brazilian seasonally dry tropical forest. *Scientific Reports*, *10*(1), 9454. https://doi.org/10.1038/s41598-020-66415-w

Merbold, L., Ardö, J., Arneth, A., Scholes, R. J., Nouvellon, Y., De Grandcourt, A., Archibald, S., Bonnefond, J.-M., Boulain, N., & Brueggemann, N. (2009). Precipitation as driver of carbon fluxes in 11 African ecosystems. *Biogeosciences*, *6*(6), 1027–1041. https://doi.org/10.5194/bg-6-1027-2009

Meza, F. J., Montes, C., Bravo-Martínez, F., Serrano-Ortiz, P., & Kowalski, A. S. (2018). Soil water content effects on net ecosystem CO_2 exchange and actual evapotranspiration in a Mediterranean semi-arid savanna of Central Chile. *Scientific Reports*, *8*(1), 8570. https://doi.org/10.1038/s41598-018-26934-z

Moncrieff, J., Clement, R., Finnigan, J., & Meyers, T. (2005). Averaging, detrending, and filtering of Eddy covariance time Series. In X. Lee, W. Massman, & B. Law (Eds.), *Handbook of micrometeorology: A guide for surface flux measurement and analysis. Atmospheric and Oceanographic Sciences Library, vol. 29* (pp. 7–31). Springer. https://doi.org/10.1007/1-4020-2265-4_2

Moncrieff, J., Massheder, J., De Bruin, H., Elbers, J., Friborg, T., Heusinkveld, B., Kabat, P., Scott, S., Soegaard, H., & Verhoef, A. (1997). A system to measure surface fluxes of momentum, sensible heat, water vapour and carbon dioxide. *Journal of Hydrology*, *188*, 589–611. https://doi.org/10.1016/S0022-1694(96)03194-0

Mortimore, M. (2010). Adapting to drought in the Sahel: Lessons for climate change. *Wiley Interdisciplinary Reviews: Climate Change*, *1*(1), 134–143. https://doi.org/10.1002/wcc.25

Mougin, É., Hiernaux, P., Kergoat, L., Grippa, M., De Rosnay, P., Timouk, F., Le Dantec, V., Demarez, V., Lavenu, F., & Arjounin, M. (2009). The AMMA-CATCH Gourma observatory site in Mali: Relating climatic variations to changes in vegetation, surface hydrology, fluxes and natural resources. *Journal of Hydrology*, *375*(1–2), 14–33. https://doi.org/10.1016/j.jhydrol.2009.06.045

Nelson, J. A., Carvalhais, N., Cuntz, M., Delpierre, N., Knauer, J., Ogée, J., Migliavacca, M., Reichstein, M., & Jung, M. (2018). Coupling water and carbon fluxes to constrain estimates of transpiration: The TEA algorithm. *Journal of Geophysical Research: Biogeosciences*, *123*(12), 3617–3632. https://doi.org/10.1029/2018JG004727

Niu, S., Xing, X., Zhang, Z., Xia, J., Zhou, X., Song, B., Li, L., & Wan, S. (2011). Water-use efficiency in response to climate change: From leaf to ecosystem in a temperate steppe. *Global Change Biology*, *17*(2), 1073–1082. https://doi.org/10.1111/j.1365-2486.2010.02280.x

Niziński, J., Ziernicka-Wojtaszek, A., Książek, L., Gawroński, K., Skowera, B., Zuśka, Z., & Wojkowski, J. (2019). Actual evapotranspiration of grasslands and plantations in arid zones. *Applied Ecology and Environmental Research*, *17*(3), 6535–6547. https://doi.org/10.15666/aeer/1703_65356547

Novick, K., Walker, J., Chan, W., Schmidt, A., Sobek, C., & Vose, J. (2013). Eddy covariance measurements with a new fast-response, enclosed-path analyzer: Spectral characteristics and cross-system comparisons. *Agricultural and Forest Meteorology*, *181*, 17–32. https://doi.org/10.1016/j.agrformet.2013.06.020

Novick, K. A., Ficklin, D. L., Grossiord, C., Konings, A. G., Martínez-Vilalta, J., Sadok, W., Trugman, A. T., Williams, A. P., Wright, A. J., & Abatzoglou, J. T. (2024). The impacts of rising vapour pressure deficit in natural and managed ecosystems. *Plant, Cell & Environment*, *47*, 3561–3589. https://doi.org/10.1111/pce.14846

Papale, D., Reichstein, M., Aubinet, M., Canfora, E., Bernhofer, C., Kutsch, W., Longdoz, B., Rambal, S., Valentini, R., & Vesala, T. (2006). Towards a standardized processing of Net Ecosystem Exchange measured with eddy covariance technique: Algorithms and uncertainty estimation. *Biogeosciences*, *3*(4), 571–583. https://doi.org/10.5194/bg-3-571-2006

Pastorello, G., Trotta, C., Canfora, E., Chu, H., Christianson, D., Cheah, Y.-W., Poindexter, C., Chen, J., Elbashandy, A., Humphrey, M., Isaac, P., Polidori, D., Reichstein, M., Ribeca, A., Van Ingen, C., Vuichard, N., Zhang, L., Amiro, B., Ammann, C., … Papale, D. (2020). The FLUXNET2015 dataset and the ONEFlux processing pipeline for eddy covariance data. *Scientific Data*, *7*(1), 225. https://doi.org/10.1038/s41597-020-0534-3

Pedregosa, F., Varoquaux, G., Gramfort, A., Michel, V., Thirion, B., Grisel, O., Blondel, M., Prettenhofer, P., Weiss, R., & Dubourg, V. (2011). Scikit-learn: Machine learning in Python. *The Journal of Machine Learning Research*, *12*, 2825–2830.

Perez-Quezada, J. F., Trejo, D., Lopatin, J., Aguilera, D., Osborne, B., Galleguillos, M., Zattera, L., Celis-Diez, J. L., & Armesto, J. J. (2024).

Comparison of carbon and water fluxes and the drivers of ecosystem water use efficiency in a temperate rainforest and a peatland in southern South America. *Biogeosciences*, *21*(5), 1371–1389. https://doi.org/10.5194/bg-21-1371-2024

Polonik, P., Chan, W., Billesbach, D., Burba, G., Li, J., Nottrott, A., Bogoev, I., Conrad, B., & Biraud, S. (2019). Comparison of gas analyzers for eddy covariance: Effects of analyzer type and spectral corrections on fluxes. *Agricultural and Forest Meteorology*, *272*, 128–142. https://doi.org/10.1016/j.agrformet.2019.02.010

Poulter, B., Frank, D., Ciais, P., Myneni, R. B., Andela, N., Bi, J., Broquet, G., Canadell, J. G., Chevallier, F., & Liu, Y. Y. (2014). Contribution of semi-arid ecosystems to interannual variability of the global carbon cycle. *Nature*, *509*(7502), 600–603. https://doi.org/10.1038/nature13376

Rahimi, J., Ago, E. E., Ayantunde, A., Berger, S., Bogaert, J., Butterbach-Bahl, K., Cappelaere, B., Cohard, J.-M., Demarty, J., & Diouf, A. A. (2021). Modeling gas exchange and biomass production in West African Sahelian and Sudanian ecological zones. *Geoscientific Model Development*, *14*(6), 3789–3812. https://doi.org/10.5194/gmd-14-3789-2021

Ramier, D., Boulain, N., Cappelaere, B., Timouk, F., Rabanit, M., Lloyd, C. R., Boubkraoui, S., Métayer, F., Descroix, L., & Wawrzyniak, V. (2009). Towards an understanding of coupled physical and biological processes in the cultivated Sahel–1. Energy and water. *Journal of Hydrology*, *375*(1–2), 204–216. https://doi.org/10.1016/j.jhydrol.2008.12.002

Rasmussen, M. O., Göttsche, F.-M., Diop, D., Mbow, C., Olesen, F.-S., Fensholt, R., & Sandholt, I. (2011). Tree survey and allometric models for tiger bush in northern Senegal and comparison with tree parameters derived from high resolution satellite data. *International Journal of Applied Earth Observation and Geoinformation*, *13*(4), 517–527. https://doi.org/10.1016/j.jag.2011.01.007

Reichstein, M., Falge, E., Baldocchi, D., Papale, D., Aubinet, M., Berbigier, P., Bernhofer, C., Buchmann, N., Gilmanov, T., Granier, A., Grunwald, T., Havrankova, K., Ilvesniemi, H., Janous, D., Knohl, A., Laurila, T., Lohila, A., Loustau, D., Matteucci, G., … Valentini, R. (2005). On the separation of net ecosystem exchange into assimilation and ecosystem respiration: Review and improved algorithm. *Global Change Biology*, *11*(9), 1424–1439. https://doi.org/10.1111/j.1365-2486.2005.001002.x

Rojas-Sandoval, J. (2016). *Balanites aegyptiaca* (simple-thorned torchwood). In C.A.B. International (Ed.), *Invasive species compendium detailed coverage of invasive species threatening. Livelihoods and the environment worldwide* (pp. 1–4). CABI.

Ross, C. W., Hanan, N. P., Prihodko, L., Anchang, J., Ji, W., & Yu, Q. (2021). Woody-biomass projections and drivers of change in sub-Saharan Africa. *Nature Climate Change*, *11*(5), 449–455. https://doi.org/10.1038/s41558-021-01034-5

Rosseel, Y. (2012). lavaan: An R package for structural equation modeling. *Journal of Statistical Software*, *48*, 1–36. https://doi.org/10.18637/jss.v048.i02

Roupsard, O., Ferhi, A., Granier, A., Pallo, F., Depommier, D., Mallet, B., Joly, H., & Dreyer, E. (1999). Reverse phenology and dry-season water uptake by *Faidherbia albida* (Del.) A. Chev. in an agroforestry parkland of Sudanese West Africa. *Functional Ecology*, *13*(4), 460–472. https://doi.org/10.1046/j.1365-2435.1999.00345.x

Ru, J., Wan, S., Hui, D., Song, J., & Wang, J. (2022). Increased interannual precipitation variability enhances the carbon sink in a semi-arid grassland. *Functional Ecology*, *36*(4), 987–997. https://doi.org/10.1111/1365-2435.14011

Ruehr, S., Keenan, T. F., Williams, C., Zhou, Y., Lu, X., Bastos, A., Canadell, J. G., Prentice, I. C., Sitch, S., & Terrer, C. (2023). Evidence and attribution of the enhanced land carbon sink. *Nature Reviews Earth and Environment*, *4*(8), 518–534. https://doi.org/10.1038/s43017-023-00456-3

Rybchak, O., du Toit, J., Delorme, J.-P., Jüdt, J.-K., Bieri, M., Midgley, G., Mukwashi, K., Thau, C., Feig, G., & Lucas-Moffat, A. (2024). Livestock grazing and biodiversity: Effects on CO_2 exchange in semi-arid Karoo ecosystems, South Africa. *Science of the Total Environment*, *910*, 168517. https://doi.org/10.1016/j.scitotenv.2023.168517

Sanni, S. A., Oluwasemire, K. O., & Nnoli, N. O. (2012). *Traditional capacity for weather prediction, variability and coping strategies in the front line states of Nigeria*. https://doi.org/10.4236/as.2012.34075

Scott, R. L., Hamerlynck, E. P., Jenerette, G. D., Moran, M. S., & Barron-Gafford, G. A. (2010). Carbon dioxide exchange in a semidesert grassland through drought-induced vegetation change. *Journal of Geophysical Research: Biogeosciences*, *115*(G3), G03026. https://doi.org/10.1029/2010JG001348

Seid, M., Kuhn, N., & Fikre, T. (2016). The role of pastoralism in regulating ecosystem services. *Revue scientifique et technique (International Office of Epizootics)*, *35*(2), 435–444. https://doi.org/10.20506/rst.35.2.2534

Sibret, T., Verbruggen, W., Peaucelle, M., Verryckt, L. T., Bauters, M., Combe, M., Boeckx, P., & Verbeeck, H. (2021). High photosynthetic capacity of Sahelian C_3 and C_4 plants. *Photosynthesis Research*, *147*(2), 161–175. https://doi.org/10.1007/s11120-020-00801-3

Sitch, S., Friedlingstein, P., Gruber, N., Jones, S. D., Murray-Tortarolo, G., Ahlström, A., Doney, S. C., Graven, H., Heinze, C., & Huntingford, C. (2015). Recent trends and drivers of regional sources and sinks of carbon dioxide. *Biogeosciences*, *12*(3), 653–679. https://doi.org/10.5194/bg-12-653-2015

Song, J., Zhou, S., Yu, B., Li, Y., Liu, Y., Yao, Y., Wang, S., & Fu, B. (2024). Serious underestimation of reduced carbon uptake due to vegetation compound droughts. *npj Climate and Atmospheric Science*, *7*(1), 23. https://doi.org/10.1038/s41612-024-00571-y

Souverijns, N., Buchhorn, M., Horion, S., Fensholt, R., Verbeeck, H., Verbesselt, J., Herold, M., Tsendbazar, N.-E., Bernardino, P. N., & Somers, B. (2020). Thirty years of land cover and fraction cover changes over the Sudano-Sahel using Landsat time series. *Remote Sensing*, *12*(22), 3817. https://doi.org/10.3390/rs12223817

Stone, E. L., & Kalisz, P. J. (1991). On the maximum extent of tree roots. *Forest Ecology and Management*, *46*(1–2), 59–102. https://doi.org/10.1016/0378-1127(91)90245-Q

Tagesson, T., Ardö, J., Guiro, I., Cropley, F., Mbow, C., Horion, S., Ehammer, A., Mougin, E., Delon, C., Galy-Lacaux, C., & Fensholt, R. (2016). Very high carbon exchange fluxes for a grazed semi-arid savanna ecosystem in West Africa. *Danish Journal of Geography*, *116*, 93–109. https://doi.org/10.1080/00167223.2016.1178072

Tagesson, T., Fensholt, R., Cappelaere, B., Mougin, E., Horion, S., Kergoat, L., Nieto, H., Mbow, C., Ehammer, A., Demarty, J., & Ardö, J. (2016). Spatiotemporal variability in carbon exchange fluxes across the Sahel. *Agricultural and Forest Meteorology*, *226*, 108–118. https://doi.org/10.1016/j.agrformet.2016.05.013

Tagesson, T., Fensholt, R., Cropley, F., Guiro, I., Horion, S., Ehammer, A., & Ardö, J. (2015). Dynamics in carbon exchange fluxes for a grazed semi-arid savanna ecosystem in West Africa. *Agriculture Ecosystems & Environment*, *205*, 15–24. https://doi.org/10.1016/j.agee.2015.02.017

Tagesson, T., Fensholt, R., & Guiro, I. (2015). Ecosystem properties of semiarid savanna grassland in West Africa and its relationship with environmental variability. *Global Change Biology*, *21*(1), 250–264. https://doi.org/10.1111/gcb.12734

Tang, X., Li, H., Desai, A. R., Nagy, Z., Luo, J., Kolb, T. E., Olioso, A., Xu, X., Yao, L., & Kutsch, W. (2014). How is water-use efficiency of terrestrial ecosystems distributed and changing on Earth? *Scientific Reports*, *4*(1), 7483. https://doi.org/10.1038/srep07483

Taylor, P. G., Cleveland, C. C., Wieder, W. R., Sullivan, B. W., Doughty, C. E., Dobrowski, S. Z., & Townsend, A. R. (2017). Temperature

and rainfall interact to control carbon cycling in tropical forests. *Ecology Letters*, *20*(6), 779–788. https://doi.org/10.1111/ele.12765

Trisos, C. H., Adelekan, I. O., Totin, E., Ayanlade, A., Efitre, J., Gemeda, A., Kalaba, K., Lennard, C., Masao, C., Mgaya, Y., Ngaruiya, G., Olago, D., Simpson, N. P., & Zakieldeen, S. (2022). Africa. In H.-O. Pörtner, D. C. Roberts, M. Tignor, E. S. Poloczanska, K. Mintenbeck, A. Alegría, M. Craig, S. Langsdorf, S. Löschke, V. Möller, A. Okem, & B. Rama (Eds.), *Climate change 2022: Impacts, adaptation and vulnerability*. Contribution of Working Group II to the sixth assessment report of the intergovernmental panel on climate change (pp. 1285–1455). Cambridge University Press.

Tucker, C. J. (1979). Red and photographic infrared linear combinations for monitoring vegetation. *Remote Sensing of Environment*, *8*(2), 127–150. https://doi.org/10.1016/0034-4257(79)90013-0

Verbruggen, W., Schurgers, G., Horion, S., Ardö, J., Bernardino, P. N., Cappelaere, B., Demarty, J., Fensholt, R., Kergoat, L., & Sibret, T. (2021). Contrasting responses of woody and herbaceous vegetation to altered rainfall characteristics in the Sahel. *Biogeosciences*, *18*(1), 77–93. https://doi.org/10.5194/bg-18-77-2021

Vicente-Serrano, S. M., McVicar, T. R., Miralles, D. G., Yang, Y., & Tomas-Burguera, M. (2020). Unraveling the influence of atmospheric evaporative demand on drought and its response to climate change. *Wiley Interdisciplinary Reviews: Climate Change*, *11*(2), e632. https://doi.org/10.1002/wcc.632

Vickers, D., & Mahrt, L. (1997). Quality control and flux sampling problems for tower and aircraft data. *Journal of Atmospheric and Oceanic Technology*, *14*(3), 512–526. https://doi.org/10.1175/1520-0426(1997)014<0512:QCAFSP>2.0.CO;2

Wang, C., Li, S., Wu, M., Zhang, W., Guo, Z., Huang, S., & Yang, D. (2023). Co-regulation of temperature and moisture in the irrigated agricultural ecosystem productivity. *Agricultural Water Management*, *275*, 108016. https://doi.org/10.1016/j.agwat.2022.108016

Wang, Y., Liu, Y., Zhou, L., & Zhou, G. (2024). Spatiotemporal patterns of phenological metrics and their relationships with environmental drivers in grasslands. *Science of the Total Environment*, *938*, 173489. https://doi.org/10.1016/j.scitotenv.2024.173489

Wang, Y., Zhou, L., Ping, X., Jia, Q., & Li, R. (2018). Ten-year variability and environmental controls of ecosystem water use efficiency in a rainfed maize cropland in Northeast China. *Field Crops Research*, *226*, 48–55. https://doi.org/10.1016/j.fcr.2018.07.006

Webb, E. K., Pearman, G. I., & Leuning, R. (1980). Correction of flux measurements for density effects due to heat and water vapour transfer. *Quarterly Journal of the Royal Meteorological Society*, *106*(447), 85–100. https://doi.org/10.1002/qj.49710644707

Wilczak, J. M., Oncley, S. P., & Stage, S. A. (2001). Sonic anemometer tilt correction algorithms. *Boundary-Layer Meteorology*, *99*, 127–150. https://doi.org/10.1023/A:1018966204465

Wutzler, T., Lucas-Moffat, A., Migliavacca, M., Knauer, J., Sickel, K., Šigut, L., Menzer, O., & Reichstein, M. (2018). Basic and extensible post-processing of eddy covariance flux data with REddyProc. *Biogeosciences*, *15*(16), 5015–5030. https://doi.org/10.5194/bg-15-5015-2018

Xue, B.-L., Guo, Q., Otto, A., Xiao, J., Tao, S., & Li, L. (2015). Global patterns, trends, and drivers of water use efficiency from 2000 to 2013. *Ecosphere*, *6*(10), 1–18. https://doi.org/10.1890/ES14-00416.1

Yang, Y., Guan, H., Batelaan, O., McVicar, T. R., Long, D., Piao, S., Liang, W., Liu, B., Jin, Z., & Simmons, C. T. (2016). Contrasting responses of water use efficiency to drought across global terrestrial ecosystems. *Scientific Reports*, *6*(1), 23284. https://doi.org/10.1038/srep23284

Yang, Z., Wei, Y., Fu, G., Xiao, R., Chen, J., Zhang, Y., Wang, D., & Li, J. (2021). Decreased precipitation in the late growing season weakens an ecosystem carbon sink in a semi-arid grassland. *Journal of Applied Ecology*, *58*(10), 2101–2112. https://doi.org/10.1111/1365-2664.13942

Yao, J., Gao, Z., Huang, J., Liu, H., & Wang, G. (2021). Uncertainties in eddy covariance CO_2 fluxes in a semiarid sagebrush ecosystem caused by gap-filling approaches. *Atmospheric Chemistry and Physics*, *21*(20), 15589–15603. https://doi.org/10.5194/acp-21-15589-2021

Zeng, Y., Jia, L., Menenti, M., Jiang, M., Barnieh, B. A., Bennour, A., & Lv, Y. (2023). Changes in vegetation greenness related to climatic and non-climatic factors in the Sudano-Sahelian region. *Regional Environmental Change*, *23*(3), 92. https://doi.org/10.1007/s10113-023-02084-5

Zhong, Z., He, B., Wang, Y.-P., Chen, H. W., Chen, D., Fu, Y. H., Chen, Y., Guo, L., Deng, Y., & Huang, L. (2023). Disentangling the effects of vapor pressure deficit on northern terrestrial vegetation productivity. *Science Advances*, *9*(32), eadf3166. https://doi.org/10.1126/sciadv.adf3166

Zhu, S., Clement, R., McCalmont, J., Davies, C. A., & Hill, T. (2022). Stable gap-filling for longer eddy covariance data gaps: A globally validated machine-learning approach for carbon dioxide, water, and energy fluxes. *Agricultural and Forest Meteorology*, *314*, 108777. https://doi.org/10.1016/j.agrformet.2021.108777

Zscheischler, J., Mahecha, M. D., Avitabile, V., Calle, L., Carvalhais, N., Ciais, P., Gans, F., Gruber, N., Hartmann, J., & Herold, M. (2017). Reviews and syntheses: An empirical spatiotemporal description of the global surface–atmosphere carbon fluxes: Opportunities and data limitations. *Biogeosciences*, *14*(15), 3685–3703. https://doi.org/10.5194/bg-14-3685-2017

SUPPORTING INFORMATION

Additional supporting information can be found online in the Supporting Information section at the end of this article.

How to cite this article: Wieckowski, A., Vestin, P., Ardö, J., Roupsard, O., Ndiaye, O., Diatta, O., Ba, S., Agbohessou, Y., Fensholt, R., Verbruggen, W., Gebremedhn, H. H., & Tagesson, T. (2024). Eddy covariance measurements reveal a decreased carbon sequestration strength 2010–2022 in an African semiarid savanna. *Global Change Biology*, *30*, e17509. https://doi.org/10.1111/gcb.17509